reported to be homogenously $CD23^{hi}CD38^{int/low}$.[5,28] The $CD23^{low}CD38^{hi}$ cell population present within hu/SCID tumors expresses lytic cycle EBV transcripts, while the $CD23^{int}CD38^{int}$ population only expresses the latent cycle transcripts EBNA-1, EBNA-2, and LMP-1.[5] We demonstrated that surface CXCR4 is predominantly expressed by the $CD23^{low}$ tumor cell subset, previously shown to have a low proliferative index and high-level Ig secretion, typical of plasma cells.[5] Thus, it is conceivable that differential expression of EBV genes could translate into modulation of chemokine receptor expression, with CXCR4 up-regulation by lytic gene products.

Given these premises, we concentrated our attention on the CXCR4 ligand, CXCL12, to evaluate whether a putative autocrine loop could be at work in the lymphomagenesis process of this experimental model. We showed for the first time that EBV-transformed B cells, both LCLs and hu/SCID tumors, are able to express CXCL12, in contrast to resting and in vitro–activated B lymphocytes. Interestingly, CXCL12 was shown to be produced predominantly by the $CD23^{int}$ tumor cell subset, which expresses low levels of surface CXCR4 (sCXCR4) but high levels of internal CXCR4. It has been previously shown that the transfer of a tumor cell line (generated after in vitro growth of hu/SCID lymphomas) expressing CD23 at intermediate levels to SCID mice entails a substantial shift to low CD23 expression. Because the former expresses low levels of sCXCR4, while the latter expresses good levels of sCXCR4, it could be inferred that the $CD23^{int}CD38^{int}sCXCR4^{low}$ (lymphoblastoid-like) subset shifts phenotype to $CD23^{low}CD38^{hi}sCXCR4^{int}$ (plasmacytoid-like) after transfer and growth in SCID mice with gain of CXCL12 responsiveness and that the plasmacytoid cells originate from the lymphoblastoid cells.[28] We thus expand the current knowledge regarding this experimental model, proposing that the differentiation of plasmacytoid cells from lymphoblastoid cells involves gain of CXCR4 surface expression (and responsiveness) and reduced production of CXCL12 and that the CXCL12/CXCR4 axis may be important in the homeostasis of the 2 tumor subsets that are found within lymphomas. Furthermore, in vitro treatment of hu/SCID lymphoma cells with neutralizing ant-CXCL12 Abs or TC14012 decreased cell survival and proliferation, implying autocrine regulation of hu/SCID lymphoma cell biology by endogenous CXCL12. However, the fact that blocking CXCR4 or CXCL12 reduced but did not completely inhibit the proliferation and survival of hu/SCID lymphoma cells suggests that factors and pathways other than CXCR4/CXCL12 interactions are involved in the regulation of these processes. Further work is warranted to clarify this issue.

Along with the demonstration that CXCL12 expression by B lymphocytes could be related to EBV transformation, one major finding of this work is the demonstration that interfering with the CXCL12/CXCR4 axis may affect EBV-transformed cell behavior, both in vitro and in vivo. Indeed, we found that the lymphomagenesis process was associated with a dramatic increase in the levels of murine CXCL12 present within the peritoneal cavity, suggesting a role for this chemokine in lymphoma growth and progression. Notably, with the ELISA kit that was used, human CXCL12 (SDF-1α) exhibits 26% to 42% cross-reactivity at all concentrations, so the contribution of human CXCL12 to tumor growth cannot be completely excluded. In vivo neutralization of the CXCL12/CXCR4 axis by a neutralizing anti-CXCL12 Ab or CXCR4 antagonist had a dramatic effect on lymphoma development, even though the anti-CXCL12 antiserum seemed more effective. The CXCR4 antagonist used in vivo was 4F-benzoyl-TN14003 instead of TC14012, because the latter has been shown to be relatively unstable in rat liver homogenates while 4F-benzoyl-TN14003 is relatively stable in vivo.[18] The minor efficacy of 4F-benzoyl-TN14003 compared with the neutralizing anti-CXCL12 Abs may reflect the greater difficulties of the former with respect to administration modality, schedule, and in vivo stability or half-life. Indeed, only high doses of this antagonist inhibited proliferation and cell survival in vitro.

The neutralization of CXCR4 through the use of an anti-CXCR4 Ab has been shown to be able to prevent tumor growth in nonobese diabetic (NOD)/SCID mice injected intraperitoneally with the Namalwa cell line[13]; however, compared with PBMC-injected SCID mice, this experimental model may be more distant from the human lymphomagenesis setting. In addition, the use of an anti-CXCR4 Ab as a tumor-preventing tool may give a less mechanistic insight into the relevance of the CXCL12/CXCR4 axis in the lymphomagenesis process; in fact, it could be argued that the effect on lymphoma growth could be due to tumor cell elimination by the mouse reticuloendothelial system. We chose to prevent this possible criticism through the use of an Ab directed against CXCL12 and a CXCR4-specific antagonist. In any case, these findings strongly suggest that the CXCR4/CXCL12 axis could play a significant role in favoring the outgrowth and dissemination of EBV-transformed cells in PBMC-injected SCID mice. Because CXCR4 expression has been proven in the human tumor counterpart of this experimental model,[13,14] the CXCL12/CXCR4 axis could indeed become an attractive target for therapy in lymphoma-bearing patients, possibly through the use of small molecular antagonists of CXCR4.

Acknowledgments

We are grateful to Dr J. Gordon (Birmingham, United Kingdom) for providing us with the CD-32L cells. We are particularly indebted to Prof R. M. Strieter (UCLA) for providing the goat anti-CXCL12 serum. We also thank Dr A. Janowska-Wieczorek (Edmonton, AB, Canada) for kind advice on the chemoinvasion assay and Dr K. Balabanian (INSERM U131, Institut Paris-Sud sur les Cytokines, Clamart, France) for help with actin polymerization experiments. Also, the great expertise of Dr A. Rosato in animal procedures is acknowledged. The invaluable help of P. Gallo in artwork preparation is gratefully acknowledged.

References

1. Rickinson AB, Kieff E. Epstein-Barr virus. In: Fields BN, Knipe DM, Howley PM, eds. Fields Virology. Philadelphia, PA: Lippincott-Raven; 2001:2511-2627.
2. Bosma GC, Custer RP, Bosma MJ. A severe combined immunodeficiency mutation in the mouse. Nature. 1983;301:527-530.
3. Custer RP, Bosma GC, Bosma MJ. Severe combined immunodeficiency (SCID) in the mouse: pathology, reconstitution, neoplasms. Am J Pathol. 1985;120:464-477.
4. Mosier DE, Gulizia RJ, Baird SM, Wilson DB. Transfer of a functional human immune system to mice with severe combined immunodeficiency. Nature. 1988;335:256-259.
5. Rochford R, Mosier DE. Differential Epstein-Barr virus gene expression in B-cell subsets recovered from lymphomas in SCID mice after transplantation of human peripheral blood lymphocytes. J Virol. 1995;69:150-155.
6. Amadori A, Veronesi A, Coppola V, Indraccolo S, Mion M, Chieco-Bianchi L. The hu-PBL-SCID mouse in human lymphocyte function and lymphomagenesis studies: achievements and caveats. Semin Immunol. 1996;8:249-254.
7. Veronese ML, Veronesi A, D'Andrea E, et al. Lymphoproliferative disease in human peripheral blood mononuclear cell-injected SCID mice, I: T

lymphocyte requirement for B cell tumor generation. J Exp Med. 1992;176:1763-1767.

8. Johannessen I, Asghar M, Crawford DH. Essential role for T cells in human B-cell lymphoproliferative disease development in severe combined immunodeficient mice. Br J Haematol. 2000;109: 600-610.
9. Piovan E, Bonaldi L, Indraccolo S, et al. Tumor outgrowth in peripheral blood mononuclear cell-injected SCID mice is not associated with early Epstein-Barr virus reactivation. Leukemia. 2003; 17:1643-1649.
10. Muller A, Homey B, Soto H, et al. Involvement of chemokine receptors in breast cancer metastasis. Nature. 2001;410:50-56.
11. Foussat A, Balabanian K, Amara A, et al. Production of stromal cell-derived factor 1 by mesothelial cells and effects of this chemokine on peritoneal B lymphocytes. Eur J Immunol. 2001;31:350-359.
12. Vicente-Manzanares M, Montoya MC, Mellado M, et al. The chemokine SDF-1alpha triggers a chemotactic response and induces cell polarization in human B lymphocytes. Eur J Immunol. 1998;28: 2197-2207.
13. Bertolini F, Dell'Agnola C, Mancuso P, et al. CXCR4 neutralization, a novel therapeutic approach for non-Hodgkin's lymphoma. Cancer Res. 2002;62:3106-3112.
14. Arai J, Yasukawa M, Yakushijin Y, Miyazaki T, Fujita S. Stromal cells in lymph nodes attract B-lymphoma cells via production of stromal cell-derived factor-1. Eur J Haematol. 2000;64:323-332.
15. Amadori A, Zamarchi R, Ciminale V, et al. HIV-1-specific B cell activation: a major constituent of spontaneous B cell activation during HIV-1 infection. J Immunol. 1989;143:2146-2152.
16. Wheeler K, Gordon J. Co-ligation of surface IgM and CD40 on naive B lymphocytes generates a blast population with an ambiguous extrafollicular/germinal centre cell phenotype. Int Immunol. 1996;8:815-828.
17. Phillips RJ, Burdick MD, Lutz M, Belperio JA, Keane MP, Strieter RM. The stromal derived factor-1/CXCL12-CXC chemokine receptor 4 biological axis in non-small cell lung cancer metastases. Am J Respir Crit Care Med. 2003;167:1676-1686.
18. Tamamura H, Hori A, Kanzaki N, et al. T140 analogs as CXCR4 antagonists identified as anti-metastatic agents in the treatment of breast cancer. FEBS Lett. 2003;550:79-83.
19. Lataillade JJ, Clay D, Bourin P, et al. Stromal cell-derived factor 1 regulates primitive hematopoiesis by suppressing apoptosis and by promoting G(0)/G(1) transition in CD34(+) cells: evidence for an autocrine/paracrine mechanism. Blood. 2002;99:1117-1129.
20. Ghia P, Transidico P, Veiga JP, et al. Chemoattractants MDC and TARC are secreted by malignant B-cell precursors following CD40 ligation and support the migration of leukemia-specific T cells. Blood. 2001;98:533-540.
21. Indraccolo S, Gola E, Rosato A, et al. Differential effects of angiostatin, endostatin and interferon-alpha(1) gene transfer on in vivo growth of human breast cancer cells. Gene Ther. 2002;9:867-878.
22. De Clerck LS, Bridts CH, Mertens AM, Moens MM, Stevens WJ. Use of fluorescent dyes in the determination of adherence of human leucocytes to endothelial cells and the effect of fluorochromes on cellular function. J Immunol Methods. 1994; 172:115-124.
23. Kijowski J, Baj-Krzyworzeka M, Majka M, et al. The SDF-1-CXCR4 axis stimulates VEGF secretion and activates integrins but does not affect proliferation and survival in lymphohematopoietic cells. Stem Cells. 2001;19:453-466.
24. Tamamura H. Development of selective antagonists against an HIV second receptor [in Japanese]. Yakugaku Zasshi. 2001;121:781-792.
25. Trentin L, Cabrelle A, Facco M, et al. Homeostatic chemokines drive migration of malignant B cells in patients with non-Hodgkin lymphomas. Blood. 2004;104:502-508.
26. Janiak M, Hashmi HR, Janowska-Wieczorek A. Use of the Matrigel-based assay to measure the invasiveness of leukemic cells. Exp Hematol. 1994;22:559-565.
27. Indraccolo S, Minuzzo S, Zamarchi R, Calderazzo F, Piovan E, Amadori A. Alternatively spliced forms of Igalpha and Igbeta prevent B cell receptor expression on the cell surface. Eur J Immunol. 2002;32:1530-1540.
28. Rochford R, Hobbs MV, Garnier JL, Cooper NR, Cannon MJ. Plasmacytoid differentiation of Epstein-Barr virus-transformed B cells in vivo is associated with reduced expression of viral latent genes. Proc Natl Acad Sci U S A. 1993;90:352-356.
29. Yokoi T, Miyawaki T, Yachie A, Kato K, Kasahara Y, Taniguchi N. Epstein-Barr virus-immortalized B cells produce IL-6 as an autocrine growth factor. Immunology. 1990;70:100-105.
30. Tosato G, Jones K, Breinig MK, McWilliams HP, McKnight JL. Interleukin-6 production in post-transplant lymphoproliferative disease. J Clin Invest. 1993;91:2806-2814.
31. Peled A, Grabovsky V, Habler L, et al. The chemokine SDF-1 stimulates integrin-mediated arrest of CD34(+) cells on vascular endothelium under shear flow. J Clin Invest. 1999;104:1199-1211.
32. Picchio GR, Kobayashi R, Kirven M, Baird SM, Kipps TJ, Mosier DE. Heterogeneity among Epstein-Barr virus-seropositive donors in the generation of immunoblastic B-cell lymphomas in SCID mice receiving human peripheral blood leukocyte grafts. Cancer Res. 1992;52:2468-2477.
33. Coppola V, Veronesi A, Indraccolo S, et al. Lymphoproliferative disease in human peripheral blood mononuclear cell-injected SCID mice, IV: Differential activation of human Th1 and Th2 lymphocytes and influence of the atopic status on lymphoma development. J Immunol. 1998;160: 2514-2522.
34. Brandes M, Legler DF, Spoerri B, Schaerli P, Moser B. Activation-dependent modulation of B lymphocyte migration to chemokines. Int Immunol. 2000;12:1285-1292.
35. Nakayama T, Fujisawa R, Izawa D, Hieshima K, Takada K, Yoshie O. Human B cells immortalized with Epstein-Barr virus upregulate CCR6 and CCR10 and downregulate CXCR4 and CXCR5. J Virol. 2002;76:3072-3077.
36. Hargreaves DC, Hyman PL, Lu TT, et al. A coordinated change in chemokine responsiveness guides plasma cell movements. J Exp Med. 2001; 194:45-56.

nature immunology

Germinal center dark and light zone organization is mediated by CXCR4 and CXCR5

Christopher D C Allen[1], K Mark Ansel[1,3], Caroline Low[1], Robin Lesley[1], Hirokazu Tamamura[2], Nobutaka Fujii[2] & Jason G Cyster[1]

Germinal center (GC) dark and light zones segregate cells undergoing somatic hypermutation and antigen-driven selection, respectively, yet the factors guiding this organization are unknown. We report here that GC organization was absent from mice deficient in the chemokine receptor CXCR4. Centroblasts had high expression of CXCR4 and GC B cells migrated toward the CXCR4 ligand SDF-1 (CXCL12), which was more abundant in the dark zone than in the light zone. CXCR4-deficient cells were excluded from the dark zone in the context of a wild-type GC. These findings establish that GC organization depends on sorting of centroblasts by CXCR4 into the dark zone. In contrast, CXCR5 helped direct cells to the light zone and deficiency in CXCL13 was associated with aberrant light zone localization.

The organization of the germinal center (GC) was described over 70 years ago based on the observation that GCs have two distinct poles or zones, called the dark and light zones based on their histological appearance[1]. These histological differences are now known to be associated with important functional differences. B cells in the dark zone, called centroblasts, undergo rounds of rapid proliferation and somatic hypermutation of their antibody variable genes. The centroblasts then become smaller, nondividing centrocytes and undergo selection in the light zone based on the affinity of their surface antibody for the inducing antigen[2]. In addition to centrocytes, the light zone contains helper T cells and a network of follicular dendritic cells (FDCs) that sequester antigen[2,3]. Centrocytes that fail to bind sufficient antigen or to receive T cell help undergo apoptotic cell death and are cleared from the GC by macrophages with tingible bodies (cellular debris)[2], whereas centrocytes that successfully bind antigen and receive T cell help survive and exit the GC as long-lived plasma cells or memory B cells[2–5].

GCs develop in a stereotypic way in B cell follicles during the first week of T cell–dependent immune responses. After an initial period of rapid B cell proliferation in the follicle, the dark zone develops proximal to the T cell zone or medullary cord region and the light zone emerges at the distal pole[6]. Once these zones are established, the proliferating centroblasts in the dark zone continuously renew the centrocytes in the light zone. Evidence for the movement of proliferating cells from the dark zone to the light zone has been provided by kinetic analyses of cells labeled with [^{3}H]thymidine or 5-bromo-2′-deoxyuridine (BrdU)[2,6,7]. Data also suggest that selected centrocytes can return to the dark zone for further rounds of division and somatic mutation[3].

Despite the extensive anatomical description of GC dark and light zones and the evidence that B cells move between these compartments, the mechanisms responsible for achieving this polarity in the GC remain a mystery. The adhesion molecules ICAM-1 and VCAM-1 are reportedly expressed in the GC and can mediate attachment of GC B cells to FDCs *in vitro* via the integrins LFA-1 and VLA-4 (refs. 8,9), but there is no evidence so far for their *in vivo* involvement in GC organization. Mice lacking the chemokine CXCL13 (BLC or BCA-1) or its receptor, CXCR5, show defects in GC size and position[10–12], but it has been unclear whether these defects are secondary to the failure of these mice to develop primary follicles and FDCs or whether they reflect a function for CXCL13 in the GC. The chemokine receptor CXCR4 is expressed on human and mouse GC B cells[13–17] and on human GC T cells[18]. However, in *in vitro* studies[13,15,17,19], GC B cells have demonstrated poor chemotactic responses to the only known CXCR4 ligand, SDF-1 (CXCL12), leading some to conclude that GC B cells have an intrinsic lack of motility.

Here we have explored the mechanisms responsible for GC organization. We demonstrate using genetic and pharmacological approaches that CXCR4 is essential for GC dark and light zone segregation. When GC B cells were rescued from rapid *in vitro* apoptosis by overexpression of the antiapoptotic Bcl-2, they showed robust chemotactic responses to SDF-1 and CXCL13. SDF-1 was expressed in GCs and was in higher abundance in the dark zone than in the light zone. Furthermore, CXCR4 more abundant centroblasts than on centrocytes and was required for centroblast localization in the dark zone. In contrast, CXCR5 helped direct cells to the CXCL13-positive light zone but it was not essential for light and dark zone segregation. However, CXCL13 and CXCR5 were

[1]Howard Hughes Medical Institute and Department of Microbiology and Immunology, University of California San Francisco, San Francisco, California 94143-0414, USA. [2]Graduate School of Pharmaceutical Sciences, Kyoto University, Sakyo-ku, Kyoto 606-8501, Japan. [3]Present address: Center for Blood Research, Harvard Medical School, 200 Longwood Avenue, Boston, Massachusetts 02115, USA. Correspondence should be addressed to J.G.C. (cyster@itsa.ucsf.edu).

Published online 1 August 2004; corrected 8 August 2004 (details online); doi:10.1038/ni1100

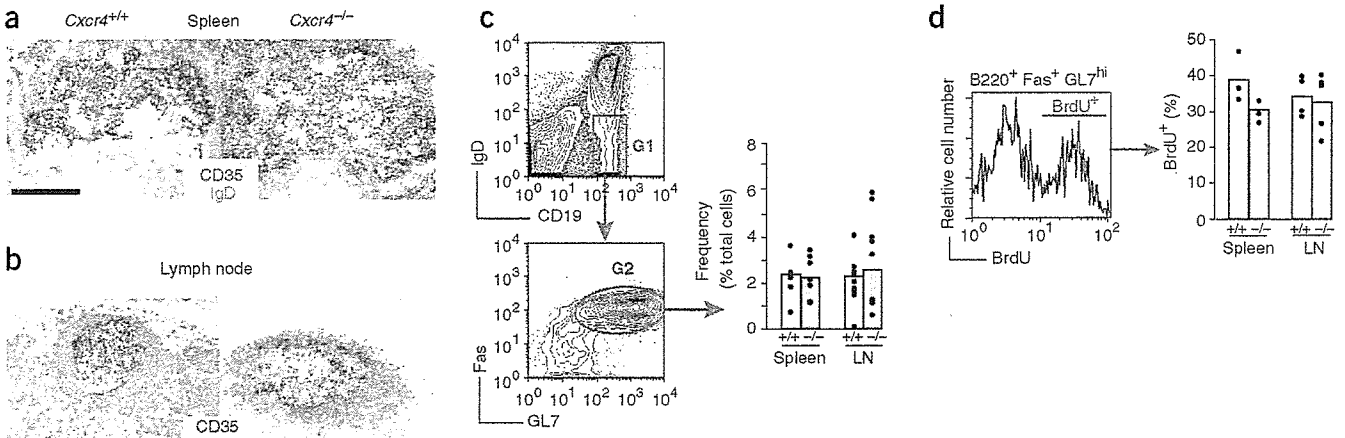

Figure 1 CXCR4 deficiency results in GC disorganization. (**a**) Immunohistochemistry of spleen GCs from immunized *Cxcr4*$^{+/+}$ or *Cxcr4*$^{-/-}$ fetal liver chimeras. Cryostat sections were stained with anti-CD35 (blue) to show the FDC network and with anti-IgD (brown) to show the IgD$^-$ GC surrounded by the IgD$^+$ follicular mantle zone. Each image is representative of GCs analyzed in four chimeras in two independent experiments. Scale bar, 100 μm. (**b**) Immunohistochemistry of lymph node GCs from immunized *Cxcr4*$^{+/+}$ or *Cxcr4*$^{-/-}$ fetal liver chimeras after 5 h of *in vivo* labeling with BrdU. Cryostat sections were stained with anti-IgD (brown) to show the surrounding follicular mantle zone; anti-CD35, FDC-M2 and anti-CD23 (all blue) for detection of the FDC network; anti-CD3 (blue) for detection of T cells; and anti-BrdU (red) for detection of proliferating centroblasts that had incorporated BrdU. Serial sections are of a single GC and are representative of GCs analyzed in three to six draining lymph nodes each from eight (CD35 and CD23), four (BrdU) or two (FDC-M2) chimeras of each type. Scale bar, 100 μm. (**c**) GC B cell frequency as percent of total organ cells, by flow cytometry. Left, GC B cells were identified as CD19$^+$IgD$^-$ cells (red box, G1) that were also GL7^{hi}Fas$^+$ (red oval, G2). Flow cytometry profiles are presented as 5% probability contour plots. In a minority of experiments, GC B cells were identified as B220$^+$GL7^{hi}PI$^-$ cells; these gating 'schemes' gave similar frequencies. Right, frequency of GC B cells as a percentage of total cells. Bars show mean and dots, individual data points. (**d**) Frequency of BrdU$^+$ GC B cells determined by flow cytometry after 5 h of *in vivo* labeling with BrdU. Red line (left) indicates BrdU$^+$ cells. Right, bars represent mean and dots, individual data points. For **c** and **d**, data points represent individual chimeras from two to three experiments. +/+, *Cxcr4*$^{+/+}$; −/−, *Cxcr4*$^{-/-}$; LN, lymph node.

required for determination of the correct position of the light zone in the GC.

RESULTS

CXCR4 is required for dark and light zone segregation

To determine whether CXCR4 is required for GC organization, we generated fetal liver chimeras by transferring wild-type (*Cxcr4*$^{+/+}$) or *Cxcr4*$^{-/-}$ fetal liver cells into lethally irradiated recipient mice. After reconstitution, we immunized these chimeras intraperitoneally with sheep red blood cells (SRBCs), a strong GC-inducing antigen, and analyzed the spleens 8 d later, at the peak of the GC response[20]. To visualize the dark and light zones of each GC, we analyzed by immunohistochemistry several cross-sections spanning more than 200 μm of depth for each spleen. In *Cxcr4*$^{+/+}$ fetal liver chimeras, GCs showed enriched staining for CD35$^+$ FDCs in the light zone, whereas in *Cxcr4*$^{-/-}$ fetal liver chimeras, GCs showed no evidence of CD35$^+$ FDC polarity; instead, the FDC network extended throughout the GC (**Fig. 1a**).

To assess whether this phenotype might represent a broad requirement for CXCR4 in GC organization, we immunized *Cxcr4*$^{-/-}$ and *Cxcr4*$^{+/+}$ fetal liver chimeras subcutaneously with antigen in adjuvant and then analyzed draining lymph nodes 10–14 d later. GCs in the lymph nodes of *Cxcr4*$^{-/-}$ fetal liver chimeras also showed disrupted organization, as assessed by staining the FDC network with antibody to CD35 (anti-CD35) and antibody FDC-M2 (**Fig. 1b**). Examination of lymph nodes also allowed us to track CD23, a marker selectively expressed on FDCs in the light zone of lymph node GCs[2,21], as seen in *Cxcr4*$^{+/+}$ fetal liver chimeras (**Fig. 1b**, left). In contrast, this marker was expressed throughout the GC in *Cxcr4*$^{-/-}$ fetal liver chimeras (**Fig. 1b**, right). In addition, the chemokine CXCL13, which is normally present in the GC light zone[22], was found throughout the GC in *Cxcr4*$^{-/-}$ fetal liver chimeras (data not shown), possibly contributing to the disrupted GC organization. These data suggest that CXCR4 is required for the formation of distinct dark and light zones.

In addition to analyzing the FDC network, we assessed the distribution of GC B cells by treating immunized chimeras with BrdU. We found that a 5-hour treatment time was optimal for preferential labeling of centroblasts in the dark zone in mouse GCs (data not shown), consistent with a previous kinetic analysis of rat GCs[6]. GCs in *Cxcr4*$^{+/+}$ fetal liver chimeras had many BrdU$^+$ cells in the dark zone and only a few labeled cells in the light zone (**Fig. 1b**, left), whereas GCs in *Cxcr4*$^{-/-}$ fetal liver chimeras had BrdU$^+$ cells uniformly distributed throughout the GC (**Fig. 1b**, right). By analyzing each GC in serial sections for the distribution of BrdU$^+$ centroblasts and CD23$^+$ FDCs, we identified dark and light zones in less than 7% of CXCR4-deficient GCs compared with more than 75% of wild-type GCs.

The requirement for CXCR4 in the GC was specific for dark and light zone segregation, as other aspects of the structure, such as size and position, were not dependent on CXCR4. Flow cytometry showed that the frequency of GC B cells was similar in *Cxcr4*$^{+/+}$ and *Cxcr4*$^{-/-}$

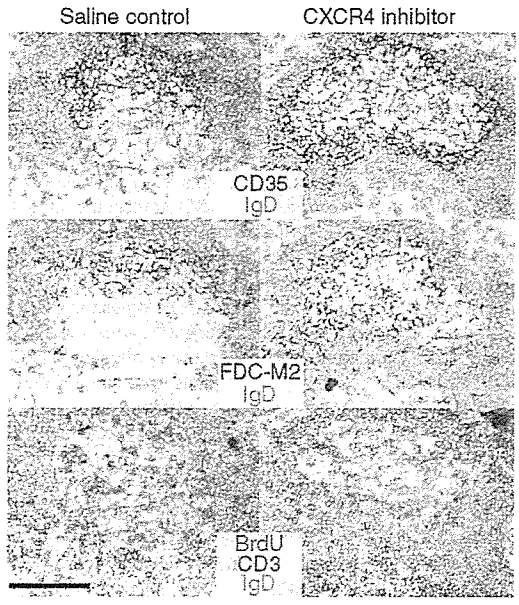

Figure 2 Treatment with a CXCR4 inhibitor results in GC disorganization. Immunohistochemistry of spleens from wild-type B6 mice immunized intraperitoneally on day 0 with SRBCs, implanted subcutaneously on day 1 with Alzet pumps containing saline (vehicle; Saline control) or the CXCR4 inhibitor 4F-benzoyl-TE14011 and analyzed 5 h after BrdU injection on day 8. Serial cryostat sections are of a single GC (antibodies used for staining, between images). Data are representative of GCs analyzed in two mice from each group. Scale bar, 100 μm.

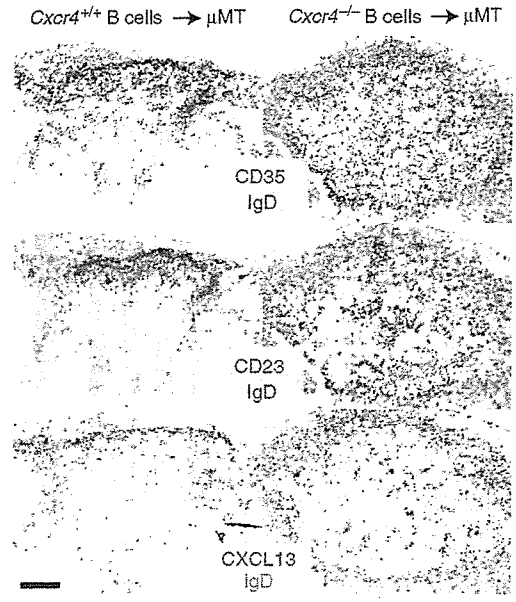

Figure 3 Deficiency of CXCR4 in B cells disrupts FDC and CXCL13 polarity in the GC. $Cxcr4^{+/+}$ or $Cxcr4^{-/-}$ B cells were purified from the spleens of fetal liver chimeras and were then transferred into B cell–deficient mice (μMT), which were immunized subcutaneously 10–11 d after transfer and analyzed 10 d after immunization. Lymph node GCs were analyzed by immunohistochemistry of cryostat sections (antibodies used for staining, between images). Serial sections are of a single GC and are representative of GCs analyzed in four mice from each group in two experiments. Scale bar, 100 μm.

fetal liver chimeras (**Fig. 1c**). Even when the reconstitution of B cells was poor in $Cxcr4^{-/-}$ fetal liver chimeras, the frequency of GC B cells was similar to that of controls (data not shown), consistent with previous reports that GC size is independent of the total number of B cells in an animal[23]. CXCR4 deficiency also did not affect the frequency of proliferating centroblasts in the GC, as determined by BrdU labeling (**Fig. 1d**). These findings further support the hypothesis that CXCR4 is specifically required for proper dark and light zone segregation of the GC.

To rule out the possibility that the disrupted GC organization in $Cxcr4^{-/-}$ fetal liver chimeras might be due to long-term defects in bone marrow development of hematopoietic cells, we administered the CXCR4 inhibitor 4F-benzoyl-TE14011 (ref. 24) to immunized normal mice for 7 d. Immunohistochemical analysis showed that GCs in these inhibitor-treated mice resembled GCs in $Cxcr4^{-/-}$ fetal liver chimeras. In spleen GCs, identification of centroblasts by BrdU labeling and visualization of FDCs by CD35 and FDC-M2 staining showed an absence of dark and light zone segregation (**Fig. 2**). Analysis of lymph node GCs by staining for CD35 and CD23 demonstrated a similar loss of GC organization after inhibitor treatment (data not shown). These results indicated that both genetic ablation and pharmacological inhibition of CXCR4 disrupted GC compartmentalization, establishing that CXCR4 is required for proper GC organization.

CXCR4 expression by B cells regulates GC organization

Although the origin of FDCs remains controversial, considerable evidence indicates that these cells are radiation resistant[22] and would therefore be wild-type in $Cxcr4^{-/-}$ fetal liver chimeras. To test whether expression of CXCR4 on B cells was required for GC organization, we purified B cells from $Cxcr4^{+/+}$ or $Cxcr4^{-/-}$ fetal liver chimeras and transferred them into B cell–deficient recipient mice (μMT) that we then immunized subcutaneously. Immunohistochemical analysis of the responding lymph nodes in the recipients showed that FDC and CXCL13 light zone polarity was typically absent in the GC when only B cells lacked CXCR4 (**Fig. 3**). To test whether expression of CXCR4 on T cells was required for GC organization, we constructed mixed irradiation chimeras by transferring a mixture of 90% T cell receptor β–deficient ($Tcrb^{-/-}$) $Tcrd^{-/-}$ bone marrow and 10% $Cxcr4^{-/-}$ fetal liver into recombination activating gene 1 (RAG1)–deficient $Rag1^{-/-}$ hosts, such that most cells would be wild-type but T cells could be derived only from the $Cxcr4^{-/-}$ fetal liver. In these chimeras, immunohistochemical analysis showed normal CD23 light zone polarity (data not shown). These data identify an essential function for CXCR4 on B cells but not T cells in normal GC organization and indicate that B cells regulate the position of FDCs and CXCL13 in the GC.

Enhanced chemotaxis of GC B cells to SDF-1

Human tonsil GC B cells express CXCR4 (refs. 13,15–17). Flow cytometric analysis of chemokine receptor surface expression on mouse GC B cells (**Fig. 4a**) showed that most GC B cells expressed 5- to 20-fold more CXCR4 than did follicular B cells. In contrast, expression of CXCR5 was similar or weakly increased (approximately twofold) and expression of CCR7, a receptor for T zone chemokines, was similar to or slightly reduced compared with that of follicular B cells (**Fig. 4a**). Although previous studies failed to find a substantial chemotactic response of freshly isolated GC B cells to lymphoid chemokines, including SDF-1 (refs. 13,15,17,19), it seemed possible that this was due to the propensity of isolated GC B cells to rapidly

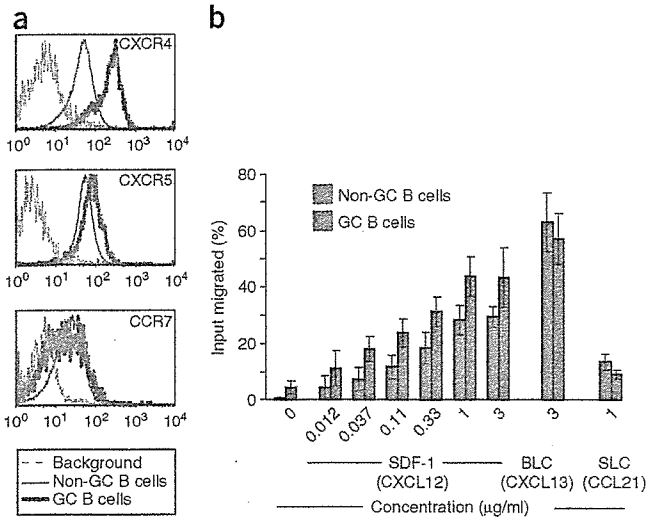

Figure 4 GC B cells upregulate CXCR4 and show enhanced chemotaxis to SDF-1. (**a**) Flow cytometric analysis of chemokine receptors for GC B cells, non-GC B cells or the following background controls: CXCR4, *Cxcr4*$^{-/-}$ GC B cells; CXCR5, *Cxcr4*$^{-/-}$*Cxcr5*$^{-/-}$ GC B cells; or CCR7, wild-type GC B cells stained with human LFA-3-Fc (staining control). Plots are representative of both spleen and lymph node data from the following immunized mice: CXCR4, 56 mice in twenty experiments; CXCR5, 21 mice in nine experiments; CCR7, 3 mice in three experiments. (**b**) Transwell migration assay of spleen cells from immunized Eμ-*Bcl2*-22 transgenic mice. Data are from four experiments with a similar overall magnitude of response and are representative of eight experiments. Bars show mean ± s.d. GC B cells show a significantly increased responsiveness to SDF-1 ($P<0.05$; 0.012–1 μg/ml) and a significantly reduced responsiveness to CCL21 ($P<0.05$) compared with non-GC B cells (Student's paired *t*-test). GC B cells were gated on a combination of the following markers: B220$^+$, CD19$^+$, GL7^{hi}, Fas$^+$ and/or IgD$^-$; non-GC B cells were gated with a combination of B220$^+$, CD19$^+$, GL7^{lo}, Fas$^-$ and/or IgD$^+$. In some experiments, dead cells were excluded by propidium iodide staining.

undergo apopotsis[2]. Indeed, in transwell migration assays with cells from immunized spleens we found that more than half of the GC B cells disappeared during the 3-hour assay, presumably by clearance mechanisms for apoptotic cells, and that the vast majority of remaining cells stained positive for annexin V and/or propidium iodide (data not shown). To overcome this rapid cell death, we used cells from mice overexpressing *Bcl2* under control of the Ig μ enhancer (Eμ-*Bcl2*-22 mice)[25]. These mice have been reported to have relatively normal GC size and morphology[26,27], and our analysis of GCs in spleens from immunized and BrdU-labeled Eμ-*Bcl2*-22 mice showed distinct centroblast and FDC clusters, consistent with normal dark and light zone segregation (**Supplementary Fig. 1** online). In transwell migration assays, transgenic *Bcl2* expression reduced the frequency of apoptotic GC B cells to less than 20% (data not shown). In contrast with previous findings, *Bcl2*-transgenic GC B cells showed enhanced migration to SDF-1 relative to that of follicular B cells, whereas migration to CXCL13 was similar and migration to a CCR7 ligand, CCL21 (SLC), was modestly reduced (**Fig. 4b**). Therefore, of the lymphoid chemokines and receptors, GC B cells have increased responsiveness to SDF-1 and increased surface expression of CXCR4, providing a further indication of involvement of this chemokine-receptor pair in the GC.

SDF-1 expression in the dark zone

SDF-1 mRNA expression has been detected by *in situ* hybridization in the splenic red pulp[28] and lymph node medullary cords[28] and in cells associated with high endothelial venules[29], but not in the GC[15,28]. Immunohistochemical analysis with two polyclonal SDF-1 antibodies showed a similar distribution of SDF-1 protein but failed to detect SDF-1 in the GC (data not shown), consistent with two previous reports that SDF-1 protein was not detected in human tonsil and lymph node GCs[30,31]. However, as the findings reported above provided strong functional evidence that SDF-1 was present in GCs, we tested whether another reagent, the monoclonal antibody K15C[32], was more sensitive in detecting SDF-1 than were the polyclonal reagents. Because K15C is a mouse antibody, we analyzed SDF-1 expression in lymphoid tissue from immunized rats. K15C produced staining that was more intense in lymph node medullary cords and high endothelial venules than did the polyclonal reagents and also

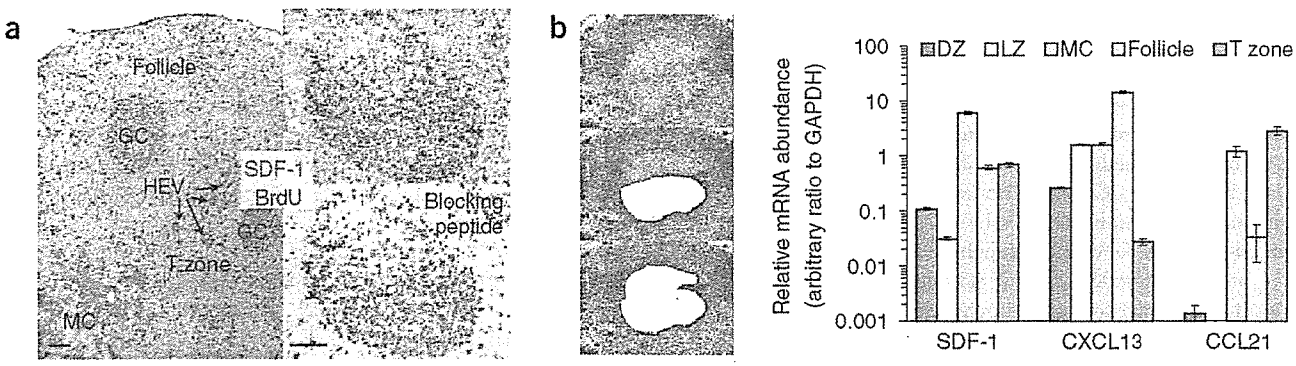

Figure 5 Detection of SDF-1 protein and mRNA in the GC. (**a**) Representative immunohistochemistry of cryostat sections of immunized rat lymph nodes stained with anti-BrdU (blue) and K15C anti-SDF-1 (red) with or without the blocking peptide. Left, low-power view; the GCs are not polarized in this plane of view. Right, serial cryostat sections in which a GC has dark and light zone polarity, as identified by BrdU labeling of centroblasts in the dark zone. Data are representative of two experiments with tissue from three rats. Scale bars, 100 μm. (**b**) Analysis of SDF-1 mRNA expression by laser-capture microdissection and quantitative RT-PCR. Top left, GC dark and light zones identified in immunized mouse lymph nodes by the respective density of methyl green staining, in which the dense cluster of large centroblasts in the dark zone produces darker staining than the loosely associated, smaller centrocytes in the light zone. Middle and bottom left, representative laser-capture microdissection (captured regions, white) of a dark zone (middle) and light zone (bottom). Right, quantitative RT-PCR analysis of mRNA expression in triplicate from one experiment (mean ± s.d.). Similar data for SDF-1 and CXCL13 were obtained in three experiments (two experiments for the T zone). HEV, high endothelial venule; MC, medullary cord; DZ, dark zone; LZ, light zone.

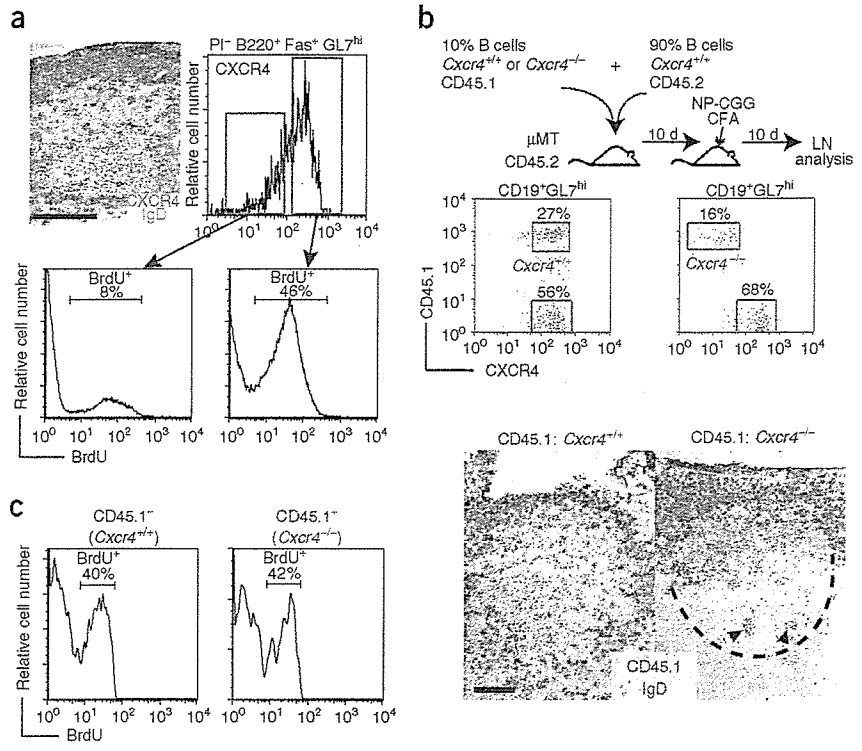

Figure 6 CXCR4 is upregulated on centroblasts and is required for dark zone localization. (**a**) CXCR4 is expressed in the dark zone by proliferating centroblasts. Top left, immunohistochemistry of a cryostat section of an immunized mouse lymph node (antibodies used for staining, bottom right), representative of four experiments. No CXCR4 staining was seen in the lymph nodes of *Cxcr4*$^{-/-}$ fetal liver chimeras (data not shown). Histograms: GC B cells (propidium iodide–negative, B220^{+}Fas^{+}GL7^{hi}) were sorted into CXCR4^{lo} and CXCR4^{hi} subsets after 5 h of *in vivo* labeling with BrdU, then were permeabilized and analyzed by flow cytometry for determination of the percentage of BrdU^{+} cells (numbers above bracketed lines). Cells were sorted from the spleens of six immunized mice; data are representative of two experiments. (**b**) CXCR4 is required for centroblasts to localize to the dark zone. For visualization of the position of *Cxcr4*$^{-/-}$ B cells in a wild-type GC, a mixture of CD45.1 (*Cxcr4*$^{+/+}$ or *Cxcr4*$^{-/-}$) and CD45.2 (*Cxcr4*$^{+/+}$) B cells were transferred into B cell–deficient mice (μMT). Flow cytometry (middle) shows the actual percentage of GC B cells (CD19^{+}GL7^{hi}) that were CD45.1^{+} in the responding lymph nodes (numbers above boxed areas, percentage of cells CD45.1^{+} or CD45.1^{-}). Bottom, the position of CD45.1^{+} cells in each GC, assessed by immunohistochemistry. The boundaries of the GCs (right, dashed lines) were determined by staining of adjacent sections with GL7 and anti-IgD (data not shown). For additional visualization of the GC region, arrowheads identify some tingible body macrophages found in the GC. Representative of five GCs each from a set of transfers. The same result was obtained in two additional experiments with mixed fetal liver chimeras. Scale bars (**a**,**b**), 100 μm. (**c**) Flow cytometry of the frequency of BrdU^{+} GC B cells in the mesenteric lymph nodes of a mixed chimera (CD45.1 *Cxcr4*$^{-/-}$ fetal liver and CD45.2 *Cxcr4*$^{+/+}$ bone marrow) that was immunized intraperitoneally and pulsed with BrdU. Histograms were gated on B220^{+}GL7^{hi} and CD45.1^{+} or CD45.1^{-} cells. Numbers above bracketed lines indicate percentage of BrdU^{+} cells. Data are representative of four chimeras in two experiments.

showed reactivity in T cell zones and B cell follicles (**Fig. 5a**, left). Moreover, K15C staining was detected in GCs, and when GC dark and light zones could be delineated distinctly by BrdU staining, the K15C signal was more intense in the dark zone than in the light zone (**Fig. 5a**, top right). We confirmed staining specificity by analyzing adjacent sections incubated with K15C in the presence of an SDF-1 peptide that encompasses the K15C epitope (thus, it acts as a blocking peptide; **Fig. 5a**, bottom right). These observations prompted us to further test whether SDF-1 mRNA could be detected in GCs. For this purpose we used laser-capture microdissection to isolate dark and light zones as well as neighboring compartments from sections of mouse lymph nodes (**Fig. 5b**). Quantitative RT-PCR analysis of RNA prepared from the captured tissue fragments showed that although the abundance was low, SDF-1 mRNA was present in the GC, with higher expression in the dark zone than in the light zone (**Fig. 5b**). SDF-1 mRNA expression in the follicle and T zone was similar and higher than in the GC and the highest expression was in medullary cords (**Fig. 5b**), an overall pattern that was similar to the K15C staining for SDF-1 protein. In contrast, CXCL13 mRNA was present in higher amounts in the light zone than the dark zone and was most abundant in follicles, consistent with previous *in situ* hybridization studies[22]. Transcripts for the T zone chemokine CCL21 were readily detected in tissue fragments isolated from the T zone but were almost undetectable in the GC dark and light zones (**Fig. 5b**). These findings demonstrate that SDF-1 is expressed in the GC and is present in higher amounts in the dark zone than in the light zone.

Dark zone localization is dependent on CXCR4

Based on our findings regarding SDF-1 distribution, we reasoned that CXCR4 might function to promote centroblast localization in the dark zone. Immunohistochemical analysis showed that CXCR4 expression was higher in the dark zone than in the light zone (**Fig. 6a**), suggesting that CXCR4 was specifically upregulated on centroblasts. We confirmed this finding by labeling proliferating centroblasts *in vivo* with BrdU, then separating CXCR4^{lo} and CXCR4^{hi} subsets of GC B cells by fluorescence-activated cell sorting (**Fig. 6a**) and analyzing the subsets by flow cytometry to determine the percentage of BrdU^{+} cells. The CXCR4^{hi} subset was enriched for the BrdU^{+} cells compared with the CXCR4^{lo} subset. Therefore, high CXCR4 expression correlates with the centroblast stage of GC B cell maturation.

The observation that CXCR4 expression was higher on centroblasts than on centrocytes was consistent with the hypothesis that SDF-1 is involved in positioning centroblasts in the dark zone. To further probe this possibility, we examined the position of *Cxcr4*$^{-/-}$ GC B cells in the context of a wild-type GC. We transferred purified *Cxcr4*$^{-/-}$ or *Cxcr4*$^{+/+}$ B cells expressing the congenic marker CD45.1 together with *Cxcr4*$^{+/+}$ CD45.2 cells into B cell–deficient mice, at a ratio such that most cells were *Cxcr4*$^{+/+}$ (**Fig. 6b**). After immunization, immunohistochemical analysis showed that CD45.1^{+} *Cxcr4*$^{-/-}$ B cells accumulated in the light zones of wild-type GCs (**Fig. 6b**, right) but were absent from the dark zone, whereas CD45.1^{+} *Cxcr4*$^{+/+}$ B cells in control recipients were evenly distributed in dark and light zones, as expected (**Fig. 6b**, left). *Cxcr4*$^{-/-}$ B cells were also absent from the dark zone of wild-type GCs in mixed chimeras generated by mixing of

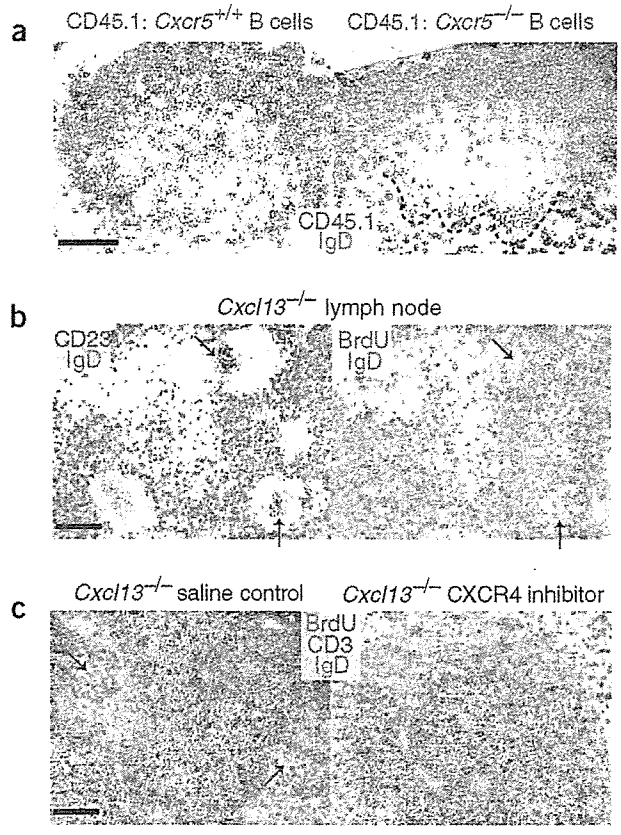

Figure 7 CXCR5 and CXCL13 function in determining light zone position. (**a**) CXCR5-deficient B cells fail to localize in the light zone of mainly wild-type GCs. A mixture of purified B cells (10% CD45.1 *Cxcr5*$^{+/+}$ plus 90% CD45.2 *Cxcr5*$^{+/+}$, or 50% CD45.1 *Cxcr5*$^{-/-}$ plus 50% CD45.2 *Cxcr5*$^{+/+}$) was transferred into B cell–deficient mice, which were then immunized and analyzed by immunohistochemistry as described in **Figure 6b**. The boundary of the dark zone (dashed lines) was identified in serial sections by staining with anti-IgD and either GL7 or anti-BrdU (data not shown). Similar GCs were noted in at least six recipients of each type in four experiments. (**b**) GCs in *Cxcl13*$^{-/-}$ mice have aberrant light zone position. GCs were analyzed by immunohistochemistry (antibodies used for staining, top left corners) of serial cryostat sections of lymph nodes present in immunized and BrdU-pulsed *Cxcl13*$^{-/-}$ mice (typically superficial cervical and mesenteric). There is dense CD23 and BrdU staining in opposing regions in two GCs. Arrows indicate the variable position of the light zone. Representative of GCs analyzed from at least three lymph nodes each from seven mice in two experiments. (**c**) CXCR4 is required for GC dark and light zone segregation in CXCL13-deficient mice. At 3 d after subcutaneous immunization, *Cxcl13*$^{-/-}$ mice were implanted with Alzet pumps containing saline (vehicle; saline control) or the CXCR4 inhibitor 4F-benzoyl-TE14011 and were analyzed on day 10 by immunohistochemistry (antibodies used for staining, between images). BrdU$^-$ regions are present in some GCs after saline treatment (left; arrows) but are absent after treatment with CXCR4 inhibitor (right). Scale bars, 100 μm.

CD45.1 *Cxcr4*$^{-/-}$ fetal liver with CD45.2 *Cxcr4*$^{+/+}$ bone marrow (data not shown). BrdU labeling indicated that a similar frequency of *Cxcr4*$^{-/-}$ and *Cxcr4*$^{+/+}$ GC B cells in these mixed chimeras were undergoing cell division (**Fig. 6c**), suggesting that both *Cxcr4*$^{-/-}$ centroblasts and centrocytes were localized in the light zone. These data establish an intrinsic requirement for CXCR4 in the dark zone localization of centroblasts.

CXCR5 determines the position of dark and light zones

The GCs in mice deficient in CXCR5 or its ligand CXCL13 have reduced size and atypical distribution[10,11], yet the function of this receptor-ligand pair in the GC has been unknown. Because CXCL13 mRNA and protein were concentrated in the GC light zone[22] (**Figs. 3 and 5b**) and GC B cells were able to migrate toward CXCL13 (**Fig. 4b**), CXCL13 and CXCR5 seemed likely to direct GC B cells to the light zone. We tested this possibility by transferring a mixture of purified CD45.1 *Cxcr5*$^{-/-}$ B cells and CD45.2 *Cxcr5*$^{+/+}$ B cells into B cell–deficient recipients and analyzing the distribution of CD45.1$^+$ cells in the GCs formed after immunization. *Cxcr5*$^{-/-}$ B cells were typically excluded from wild-type GCs (data not shown); however, after transferring larger numbers of these cells and analyzing many GCs, we noted that they were occasionally present in wild-type GCs. In these GCs, the *Cxcr5*$^{-/-}$ cells accumulated in the dark zone adjacent to the T zone and were absent from the light zone (**Fig. 7a**, right). These findings support the conclusion that CXCR5 and CXCL13 contribute to attracting GC B cells to the light zone.

Unexpectedly, however, immunohistochemical analysis of the small GCs that developed in the lymph nodes of immunized and BrdU-pulsed *Cxcl13*$^{-/-}$ mice demonstrated separate BrdU$^+$ and CD23$^+$ regions, indicating the presence of dark and light zones, in more than 66% of GCs (42 of 64; **Fig. 7b**). The relative positions of these zones were atypical, such that the light zone seemed to have a random orientation rather than being located distal to the T zone (**Fig. 7b**). Indeed, in many cases (19 of 64), CD23 staining was brightest at the center of the GC and was surrounded by a ring of BrdU$^+$ centroblasts (**Fig. 7b**). We obtained similar findings by analyzing GCs in *Cxcr5*$^{-/-}$ mice (data not shown). To investigate whether CXCR4 was responsible for the segregation of dark and light zones in the absence of CXCL13 or CXCR5, we analyzed GCs in *Cxcr4*$^{-/-}$*Cxcr5*$^{-/-}$ double-deficient fetal liver chimeras and in *Cxcl13*$^{-/-}$ or *Cxcr5*$^{-/-}$ mice treated with the CXCR4 inhibitor 4F-benzoyl-TE14011. For reasons that are unclear, expression of the FDC marker CD23 was weak in the GCs that formed in either of these conditions, such that its distribution could not be assessed, making it difficult to examine dark and light zone segregation (data not shown). However, labeling with BrdU alone showed that centroblasts formed an identifiable dark zone in about 40% (23 of 61) of GCs analyzed in *Cxcl13*$^{-/-}$ or *Cxcr5*$^{-/-}$ mice, whereas less than 10% (5 of 51) of GCs showed any polarity when CXCR4 was also deficient (**Fig. 7c** and data not shown). Overall, these data suggest that CXCR4 provides a dominant cue for GC dark and light zone segregation and that CXCR5 and CXCL13 are required for the correct orientation of these zones.

DISCUSSION

The findings reported here have identified essential requirements for GC polarization into dark and light zones. GC B cells were highly motile, and centroblasts expressed more CXCR4 than did centrocytes and localized to the GC dark zone in a CXCR4-dependent way. Consistent with this CXCR4 requirement, SDF-1 was more abundant in the GC dark zone than in the GC light zone. GC B cells also expressed CXCR5 and responded to CXCL13, a chemokine present in the GC light zone, and CXCL13 and CXCR5 'dictated' the orientation of GC light and dark zones. In addition, our analysis of mice containing CXCR4-deficient B cells indicated that B cells were involved in regulating the differential distribution of FDCs in GC light and dark zones.

It has been suggested that GC B cells do not respond or respond poorly to chemokines, based on the failure of human tonsil GC B cells to migrate in *in vitro* studies[13,15,17,19]. Instead, we found that when mouse GC B cell survival was extended by *Bcl2* overexpression, these

cells showed robust migratory responses to chemokines. Consistent with an important function for SDF-1 and CXCR4 in the GC, GC B cells responded more strongly to SDF-1 and expressed more CXCR4 than did follicular B cells. In addition, the basal motility of GC B cells was higher than that of follicular B cells when examined in the absence of chemokine. A previous study of mouse Peyer's patch GC B cells also provided evidence that the cells could respond to lymphoid chemokines, although responsiveness to SDF-1 was suggested to be reduced compared with that of follicular B cells[14], a difference most likely attributable to the effects of the rapid death of unprotected GC B cells *in vitro*. Consistent with CXCR4 also functioning in human GCs, CXCR4 has been identified on human tonsil GC B cells by flow cytometry and immunofluorescence analysis of tissue sections[13,15–17]. Moreover, human follicular lymphoma cells, which are thought to be derived from GC B cells that acquire mutations promoting increased survival, show notable chemotaxis to SDF-1 (ref. 19).

Previous studies of SDF-1 distribution have failed to detect SDF-1 mRNA or protein in GCs[15,28,30,31]. By both *in situ* hybridization and analysis of protein distribution with various polyclonal anti-SDF-1 reagents, we were also unable to detect SDF-1 in GCs. However, the sensitivity of these techniques was poor and did not exclude the possibility that SDF-1 was present in GCs in low amounts. Indeed, using more sensitive approaches, we detected a broad distribution of SDF-1 mRNA and protein in lymphoid tissues, including in GCs, follicles and T zones. Although the abundance of SDF-1 in the GC was lower than in the surrounding compartments, SDF-1 amounts in the GC dark zone were higher than in the adjacent GC light zone. The overlapping SDF-1 mRNA and protein distribution indicated that the chemokine was produced locally. Because we have not detected SDF-1 mRNA in GC B cells (data not shown), we hypothesize that SDF-1 is produced by stromal cells in the dark zone. Given these findings, along with the observation that centroblasts have higher expression of CXCR4 than do centrocytes and that CXCR4 is required for GC B cells to locate in the dark zone of wild-type GCs, we conclude that SDF-1 acts to attract or retain centroblasts in the dark zone.

Despite the higher expression of SDF-1 in the follicular mantle zone than in the adjacent GC light zone, the follicular SDF-1 does not seem to reach the light zone. This suggests that SDF-1 is bound tightly at or near sites of production, a scenario that is supported by the similar profiles of SDF-1 mRNA and protein distribution throughout the lymphoid tissue. Alternatively, boundaries may exist between the GC and surrounding compartments that limit the entry of chemokines. An implication of these findings is that chemokine function can be highly localized such that adjacent tissue regions can use the same chemokine to control distinct positional events.

CXCL13 has a distribution in the GC opposite to that of SDF-1, being more abundant in the light zone than in the dark zone. Consistent with this distribution, our mixed B cell transfer experiments indicate that CXCL13 and CXCR5 function to direct B cells to the light zone. We therefore propose that as centroblasts downregulate CXCR4 and differentiate into centrocytes, the balance of chemokine responsiveness shifts in favor of CXCL13 and the cells migrate to the light zone. Unexpectedly, CXCL13 was not essential for dark and light zone segregation, as the small GCs that developed in CXCL13-deficient mice often contained both zones. However, another defect emerged in these mice: correct polarity of the GC was lost, such that the light zone was often found in the center of the GC or near the T zone. Therefore, our findings define a function for CXCL13 in promoting the positioning of the light zone in the pole of the GC distal to the T zone, and they indicate that separation of centrocytes from centroblasts is not mediated solely by migration of centrocytes to CXCL13. Instead, as dark and light zone formation continued to be CXCR4 dependent in the absence of CXCL13 (or CXCR5), it seems that differential responsiveness to SDF-1 may be sufficient to segregate centroblasts from centrocytes.

Although we have established essential functions for the CXCR4–SDF-1 and CXCR5-CXCL13 receptor-ligand pairs in the GC, our studies also lead us to propose that further guidance factors contribute to GC organization. This hypothesis is supported by the continued formation of GC clusters in mice lacking both CXCR4 and CXCL13 function. Studies done several decades ago provided evidence that transferred radiolabeled GC B cells home selectively to GCs in recipient animals[33]. As neither SDF-1 nor CXCL13 is GC specific, these observations are best explained by the existence of a GC-specific attractant. A GC-specific activity may also help keep GC cells in a tight cluster and prevent them from migrating out of the GC into the adjacent SDF-1-, CXCL13- and CCL21-rich compartments.

Although our studies demonstrate the importance of high CXCR4 expression on centroblasts, the mechanism for selective CXCR4 upregulation on these cells remains unclear. Challenging the idea of a transcriptional mechanism, a previous study showed by RNase protection assay that CXCR4 mRNA expression was similar in GC B cells and follicular B cells from immunized mouse lymph nodes[34], and using real-time PCR we have obtained similar results for sorted splenic GC B cells (data not shown). It therefore seems likely that CXCR4 is regulated in GC B cells by post-translational mechanisms. Consistent with this possibility, several modes of CXCR4 post-translational regulation have been described[35,36].

The finding that deficiency of CXCR4 specifically in B cells disrupted the organization of GC FDCs indicates that B cells are essential in GC organization. In contrast, CXCR4 deficiency in T cells was not found to disrupt GC organization, although we have not excluded the possibility of an effect of CXCR4 on T cell localization or interactions in the GC. Compared with primary follicle FDCs, GC FDCs in the light zone normally acquire additional markers, including CD23, FcγRII and VCAM-1 (refs. 2,21,22,37). Our finding that disruption of centroblast and centrocyte segregation resulted in the appearance of $CD23^+$ FDCs throughout the GC, rather than selectively in the light zone, suggests that centrocytes in the light zone normally act to promote the development of FDCs with these unique surface markers at that pole.

In conclusion, we have established that CXCR4 upregulation on centroblasts segregates these cells from centrocytes, resulting in the establishment of the GC dark and light zones. CXCL13 and CXCR5 are important in the correct positioning of these zones and contribute to recruiting cells to the light zone. The involvement of chemokines and their receptors in guiding cell movements in the GC and the high motility of GC B cells provide a basis for understanding how newly mutated GC B cells achieve efficient encounters with antigen-bearing FDCs and antigen-specific GC T cells. This study places the GC among a growing number of processes in the immune system that are dependent on CXCR4, including B cell development[38–40], T cell development[41,42], lymph node entry[29], plasma cell localization[28] and homing of neutrophils to the bone marrow[43]. The central role of CXCR4 and SDF-1 in these diverse processes supports the view that SDF-1 is a 'primordial' chemokine[44]. It also suggests another immune function that is likely to be disrupted in patients with WHIM syndrome (warts, hypogammaglobulinemia, infections and myelokathexis) who carry C-terminal truncation mutations in CXCR4 (ref. 45) and raises new concerns about the effects of global CXCR4 inhibition for antiretroviral therapy.

METHODS

Mice, rats and chimeras. C57BL/6 (B6) and B6-CD45.1 mice were obtained from The Jackson Laboratory or the National Cancer Institute. B6-SCID mice (001913; *Prkdc*^{scid}), B6-RAG mice (002216; *Rag1*^{tm1Mom}), B6-μMT mice (002288; *Igh-6*^{tm1Cgn}) and B6-TCRβδ$^{-/-}$ mice (002122; *Tcrb*^{tm1Mom}*Tcrd*^{tm1Mom}) were from The Jackson Laboratory and were maintained on water containing 0.25–2 mg/ml of tetracycline (Sigma-Aldrich, American Livestock Company or USB). The 129-RAG (*RAG2-M*) mice were from Taconic. *Cxcr4*$^{+/-}$ mice[40] were backcrossed at least six generations to B6 and *Cxcl13*$^{-/-}$ mice[11], *Cxcr5*$^{-/-}$ mice[12] and Eμ-*Bcl2*-22 mice[25] were backcrossed at least ten generations to the B6 strain. All mice were maintained in transgenic barrier facilities. Sprague-Dawley rats were obtained from Charles River Laboratories and were maintained in a conventional facility. Protocols were approved by the Institutional Animal Care and Use Committee of the University of California San Francisco.

Fetal liver chimeras were generated as described[28] with the following modifications: as an additional method of screening for *Cxcr4* genotype, fetal liver cells were stained with biotin-conjugated antibody to CXCR4 (anti-CXCR4) followed by fluorescein isothiocyanate (FITC)-conjugated anti-CD45.1 or anti-CD45.2, phycoerythrin-conjugated anti-B220 and streptavidin-allophycocyanin and were analyzed by flow cytometry as described below. Dead cells were excluded with 1 μg/ml of propidium iodide (Sigma-Aldrich). In most experiments, fetal liver chimeras were generated in B6-SCID, B6-RAG or 129-RAG recipients to avoid a contribution from residual host lymphocytes. B6-SCID mice were irradiated with a single dose of 400 rads and B6-RAG mice were irradiated with two doses of 450 rads. After the *Cxcr4*$^{+/-}$ mice were backcrossed more than ten generations to the B6 strain, it was necessary to increase the number of *Cxcr4*$^{-/-}$ fetal liver cells transferred to at least 5×10^6 live cells per recipient to obtain reasonable B cell reconstitution frequencies (within threefold of normal). Data include only results from chimeras that had a peripheral B cell frequency of at least 6% of total lymphocytes (average: *Cxcr4*$^{+/+}$ fetal liver chimeras, 46%; *Cxcr4*$^{-/-}$ fetal liver chimeras, 18%).

Immunizations and BrdU treatment. For induction of spleen GCs, mice were immunized intraperitoneally with SRBCs (Colorado Serum Company) as described[20] and were analyzed 8 d later. For induction of lymph node GCs, animals were immunized subcutaneously in the scruff of the neck, shoulders, flanks and/or above the tail with (4-hydroxy-3-nitrophenyl)acetyl-chicken gamma globulin (mice, total of 100–200 μg; rats, total of 1.5 mg; NP_{21}-CGG or NP_{36}-CGG; Biosearch Technologies) emulsified in complete Freund's adjuvant (Sigma-Aldrich). Draining lymph nodes (superficial cervical, axillary, brachial and inguinal) were analyzed 10–14 d later. For labeling of centroblasts, BrdU (Sigma-Aldrich) in PBS (mice, 2.5 mg; rats, 7 mg) was administered by intraperitoneal injection 5–6 h before animals were killed.

CXCR4 inhibitor treatment. Alzet osmotic pumps (7-day duration, 0.5 μl/h pumping rate; Model 1007D; Durect Corporation) were loaded with 40 mg/ml of the CXCR4 antagonist 4F-benzoyl-TE14011 (ref. 24) in saline and were implanted subcutaneously in the back according to the manufacturer's instructions. As an analgesic after surgery, 0.05–0.1 mg/kg of buprenorphine (Sigma-Aldrich) was given subcutaneously.

Flow cytometry and cell sorting. Cell suspensions were prepared from spleens and lymph nodes by mechanical disruption on 70-μm nylon cell strainers (Falcon) in RPMI 1640 medium (Cellgro) containing L-glutamine, 2% FBS (Gibco-BRL), antibiotics (50 IU/ml of penicillin and 50 μg/ml of streptomycin; Cellgro) and 10 mM HEPES (Cellgro), then were washed and kept on ice. For flow cytometry, cells were plated at a density of 5×10^5 to 1×10^6 cells per well in 96-well U-bottomed plates (Falcon), were stained for 20–60 min on ice with antibodies (**Supplementary Table 1** online) in 25 μl of PBS containing 2% FBS, 1 mM EDTA and 0.1% NaN_3, and were washed twice with 200 μl of this buffer after each step. Data were collected on a Becton Dickinson FACSCalibur and were analyzed with CellQuest Pro software (Becton Dickinson) or FlowJo software (TreeStar). CCR7 was stained with CCL19-Fc as described[28], except that binding was detected with biotin-conjugated goat anti-human IgG, Fcγ fragment specific (Jackson ImmunoResearch). Annexin V staining for apoptotic cells was with annexin V–biotin (BD Pharmingen) in buffer containing Ca^{2+} and Mg^{2+} and lacking EDTA. Biotinylated reagents were detected with streptavidin-allophycocyanin (Molecular Probes). In some cases, dead cells were excluded with 1 μg/ml of propidium iodide.

For cell sorting, cell suspensions were first prepared from spleens in HBSS (UCSF Cell Culture Facility) containing 0.5% FBS, 0.5% fatty acid–free bovine serum albumin (BSA; Calbiochem) and 200 μg/ml of DNase I from bovine pancreas (Sigma-Aldrich) and were washed. Cells at a density of 4×10^7 cells/ml were labeled for 30 min on ice with biotin-conjugated anti-CXCR4, and then erythrocytes were lysed by centrifugation at 4 °C in a solution of Tris-buffered NH_4Cl. Next, cells were labeled on ice with FITC-conjugated GL7 antibody, phycoerythrin-indotricarbocyanine (Cy7)–conjugated anti-Fas, streptavidin-allophycocyanin and allphycocyanin-Cy7–conjugated anti-B220 and were washed. Dead cells were excluded with 1 μg/ml of propidium iodide. Cells were sorted on a MoFlo (DakoCytomation).

The percentage of cells that had incorporated BrdU during DNA synthesis was determined by flow cytometry as described[46] with the following modifications: 5×10^5 Jurkat cells were added to each sample to help pellet the cells; these could be excluded during analysis based on their large scatter characteristics. For mixed chimeras, cells were stained for 1 h with biotin-conjugated anti-CD45.1. After fixation and permeabilization, cells were stained in PBS containing 0.5% Tween-20 and 2% FBS with a diluted mixture of FITC-conjugated GL7, phycoerythrin-conjugated anti-BrdU, either phycoerythrin-Cy7–conjugated anti-Fas or peridinine chlorophyll protein–conjugated anti-B220, and either allophycocyanin-conjugated anti-B220 or streptavidin-allophycocyanin, or for sorted cells that were already surface stained, with phycoerythrin-conjugated anti-BrdU only.

B cell purification and transfer. Spleens were mechanically dissociated on 70-μm nylon cell strainers or, in later experiments, were digested with collagenase and EDTA as described for dendritic cells[47], as this enzymatic digestion improved B cell recovery. Splenocytes were washed and resuspended in DMEM medium (Cellgro) containing 4.5 g/l of glucose, L-glutamine, 10% FBS, 10 mM HEPES, antibiotics and 50 μg/ml of DNase I. Non–B cells were labeled for 25 min on ice with biotin-conjugated anti-CD43 (S7; BD Pharmingen) and biotin-conjugated anti-CD11c (HL3; BD Pharmingen), then were washed and centrifuged with Tris-buffered NH_4Cl for lysis of erythrocytes, and then were labeled for 20 min on ice with streptavidin microbeads (Miltenyi Biotec). Samples were depleted of labeled cells by autoMACS (Miltenyi Biotec) according to the manufacturer's instructions, resulting in a B cell purity of at least 90%, as determined by flow cytometry. T cell contamination was less than 0.75%, although the identity of the remaining cells remained unclear (they did not stain positive for CD3, CD11c, Mac-1 or NK1.1). B cells (1.5×10^7 to 4.5×10^7 per recipient) were transferred by intravenous injection into the tail veins of B cell–deficient mice (μMT).

Immunohistochemistry. Spleens and lymph nodes were placed in Tissue-Tek optimum cutting temperature compound (Sakura), were 'snap-frozen' in dry ice and ethanol and were stored at −80°C. For immunohistochemistry, cryostat sections (7 μm in thickness) were affixed to multispot (Hendley-Essex) or Superfrost/Plus (Fisher Scientific) microscope slides, dried at 20–25 °C, fixed in cold acetone for 10 min and then dried at 20–25 °C. Slides were rehydrated in Tris-buffered saline (TBS), pH 7.6, and then were stained for 2–3 h at 20–25 °C in a humidified chamber in TBS containing 0.1% BSA (ICN), 1% normal mouse serum (Sigma-Aldrich) and a diluted mixture of two primary antibodies (**Supplementary Table 2** online). After slides were washed in TBS for 3 min with gentle agitation, sections were stained for 1–2 h as described above with secondary antibodies (**Supplementary Table 3** online). Biotinylated antibodies were detected with streptavidin–alkaline phosphatase (Jackson Immunoresearch or Vector Labs). Rat tissue was stained for 18 h at 4 °C as described above in TBS containing 0.1% BSA and 1% normal rat serum with 20 μg/ml of mouse monoclonal anti-SDF-1 (K15C[32]) with or without an eightfold molar excess (2 μg/ml) of the blocking peptide KPVSLSYRSPSRFFE (synthesized by SynPep), then was stained for 2 h at 20–25 °C with biotin-conjugated goat anti-mouse IgG, Fcγ fragment specific (Jackson ImmunoResearch), followed by incubation for 1–2 h at 20–25 °C with streptavidin–ABC–alkaline phosphatase (Vector Labs). Enzyme conjugates were developed as described[46] and slides were mounted in Crystal/Mount (Biomeda). Images were collected and processed as described[48]. For detection of cells that had incorporated BrdU in sections, slides were first stained by standard immunohistochemistry as

described above and then were treated as described[46] with the following modifications: HCl treatment was for 9 min and BrdU detection was with FITC-conjugated anti-BrdU (3D4, BD Pharmingen) followed by alkaline phosphatase–conjugated anti-fluorescein.

Laser-capture microdissection and quantitative RT-PCR analysis. Lymph nodes were frozen in optimum cutting temperature compound as described above. Cryostat sections (7 μm in thickness) were affixed to glass foil slides for membrane-based laser microdissection (Leica), allowed to dry for 30 min at 20–25 °C, fixed for 1 min in 70% ethanol, washed for 30 s in distilled water, stained for 1 min with 0.6% (weight/volume) methyl green (Fluka), rinsed in distilled water, dehydrated by a graded ethanol series (70%, 95% and 100%) for 1 min each and allowed to air dry at 20–25 °C for 7–12 h. The following regions were isolated by laser-capture microdissection on a Leica AS LMD for each experiment: GC dark and light zones ($n = 40$–85), medullary cord regions ($n = 20$–40), primary follicles lacking GCs ($n = 30$–60), and T cell zones ($n = 15$–30). Microdissected regions were collected in the caps of 0.2-ml, thin-walled, RNase-free PCR tubes (Ambion). RNA was isolated with the RNeasy Micro Kit (Qiagen) with 'on-column' DNase treatment according to the manufacturer's instructions. First-strand cDNA was synthesized from RNA with Moloney murine leukemia virus reverse transcriptase (Promega) and random primers (Promega) according to the manufacturer's instructions. For quantitative PCR, 4–8% of the cDNA was placed in a final volume of 50 μl containing 1 × PCR Buffer II (Applied Biosystems, ABI), 5.5 mM $MgCl_2$ (ABI), 300 nM of each dNTP (PCR grade; Invitrogen), 1.25 units of AmpliTaq Gold DNA Polymerase (ABI) and primers and probes (**Supplementary Table 4** online). Samples were analyzed on a Prism 7900HT (ABI) with the following thermal cycler conditions: 50 °C for 2 min and 95 °C for 10 min, and then 40 cycles of 95 °C for 15 s followed by 60 °C for 1 min. For quantification of the relative amount of starting mRNA in each sample, standard curves were generated for each primer-probe set by preparation of serial dilutions of a pooled mixture containing 4% of the cDNA prepared from each microdissected region, in duplicate wells, and analysis with SDS 2.1 software (ABI). The quantity of target gene determined for each sample was divided by the quantity of a housekeeping gene (*Gapd*), giving a relative ratio of mRNA expression.

Chemotaxis assays. Cell suspensions were prepared by mechanical disruption of spleens on 70-μm cell strainers (Fisher), and erythrocytes were lysed for 2 min at 20–25 °C with Tris-buffered NH_4Cl. Splenocytes were resuspended at a density of 1×10^7 cells per ml in RPMI 1640 medium containing L-glutamine, antibiotics, 10 mM HEPES buffer and 0.5% fatty acid–free BSA. Cells were resensitized for 30–60 min at 37 °C before being plated in Transwell inserts with a pore size of 5 μm and a diameter of 6.5 mm in 24-well plates (93421; Corning Costar). For these experiments, 100 μl cells (1×10^6) were added to the upper wells and 580 μl diluted chemokine was placed in the bottom wells at the indicated concentrations (**Fig. 4b**), and plates were incubated for 3 h at 37 °C in 5% CO_2. Migrated cells were counted by flow cytometry as described[47]. Duplicate wells were analyzed for each concentration of chemokine. Recombinant human SDF-1 was from Peprotech and recombinant mouse CXCL13 and CCL21 were from R&D Systems.

Note: Supplementary information is available on the Nature Immunology website.

ACKNOWLEDGMENTS

We thank D. Hargreaves, Y. Xu and M. Lesneski for technical assistance; C. Miller for training in laser-capture microdissection; J. Dietrich for surgical expertise; S. Jiang for cell sorting; D. Littman for *Cxcr4*$^{+/-}$ mice; M. Lipp for *Cxcr5*$^{-/-}$ mice; T. Roach for some Eμ-*Bcl2*-22 mice; F. Arenzana-Seisdedos for K15C antibody; J. Lin and other members of the Weiss Lab for Jurkat cells; the Werb lab for the use of equipment and supplies; the University of California San Francisco Diabetes Center for use of the ABI Prism 7900HT; S. Luther, T. Okada and G. Cinamon for advice and comments on the manuscript; and M. Matloubian, C. Lo and J. Cholfin for discussions. Work supported by Howard Hughes Medical Institute and grants AI40098 and AI45073 from the National Institutes of Health, and by predoctoral grants from Howard Hughes Medical Institute (C.D.C.A. and K.M.A.).

COMPETING INTERESTS STATEMENT

The authors declare that they have no competing financial interests.

Received 16 March; accepted 25 June 2004
Published online at http://www.nature.com/natureimmunology/

1. Röhlich, K. Beitrag zur Cytologie der Keimzentren der Lymphknoten. *Z. Mikrosk. Anat. Forsch.* **20**, 287–297 (1930).
2. MacLennan, I.C. Germinal centers. *Annu. Rev. Immunol.* **12**, 117–139 (1994).
3. Kelsoe, G. Life and death in germinal centers (redux). *Immunity* **4**, 107–111 (1996).
4. McHeyzer-Williams, M.G. & Ahmed, R. B cell memory and the long-lived plasma cell. *Curr. Opin. Immunol.* **11**, 172–179 (1999).
5. Berek, C., Berger, A. & Apel, M. Maturation of the immune response in germinal centers. *Cell* **67**, 1121–1129 (1991).
6. Liu, Y.J., Zhang, J., Lane, P.J., Chan, E.Y. & MacLennan, I.C. Sites of specific B cell activation in primary and secondary responses to T cell-dependent and T cell-independent antigens. *Eur. J. Immunol.* **21**, 2951–2962 (1991).
7. Koburg, E. in *Germinal Centers in Immune Responses.* (eds. Cottier, H., Odartchenko, N, Schindler, R. & Congdon, C.C.) 177–182 (Springer-Verlag, New York, University of Bern, Switzerland; 1966).
8. Koopman, G. *et al.* Adhesion of human B cells to follicular dendritic cells involves both the lymphocyte function-associated antigen 1/intercellular adhesion molecule 1 and very late antigen 4/vascular cell adhesion molecule 1 pathways. *J. Exp. Med.* **173**, 1297–1304 (1991).
9. Freedman, A.S. *et al.* Adhesion of human B cells to germinal centers in vitro involves VLA-4 and INCAM-110. *Science* **249**, 1030–1033 (1990).
10. Voigt, I. *et al.* CXCR5-deficient mice develop functional germinal centers in the splenic T cell zone. *Eur. J. Immunol.* **30**, 560–567 (2000).
11. Ansel, K.M. *et al.* A chemokine-driven positive feedback loop organizes lymphoid follicles. *Nature* **406**, 309–314 (2000).
12. Forster, R. *et al.* A putative chemokine receptor, BLR1, directs B cell migration to defined lymphoid organs and specific anatomic compartments of the spleen. *Cell* **87**, 1037–1047 (1996).
13. Roy, M.P., Kim, C.H. & Butcher, E.C. Cytokine control of memory B cell homing machinery. *J. Immunol.* **169**, 1676–1682 (2002).
14. Bowman, E.P. *et al.* Developmental switches in chemokine response profiles during B cell differentiation and maturation. *J. Exp. Med.* **191**, 1303–1318 (2000).
15. Bleul, C.C., Schultze, J.L. & Springer, T.A. B lymphocyte chemotaxis regulated in association with microanatomic localization, differentiation state, and B cell receptor engagement. *J. Exp. Med.* **187**, 753–762 (1998).
16. Forster, R. *et al.* Intracellular and surface expression of the HIV-1 coreceptor CXCR4/fusin on various leukocyte subsets: rapid internalization and recycling upon activation. *J. Immunol.* **160**, 1522–1531 (1998).
17. Casamayor-Palleja, M., Mondiere, P., Verschelde, C., Bella, C. & Defrance, T. BCR ligation reprograms B cells for migration to the T zone and B-cell follicle sequentially. *Blood* **99**, 1913–1921 (2002).
18. Estes, J.D. *et al.* Follicular dendritic cell-mediated up-regulation of CXCR4 expression on CD4 T cells and HIV pathogenesis. *J. Immunol.* **169**, 2313–2322 (2002).
19. Corcione, A. *et al.* Stromal cell-derived factor-1 as a chemoattractant for follicular center lymphoma B cells. *J. Natl. Cancer Inst.* **92**, 628–635 (2000).
20. Shinall, S.M., Gonzalez-Fernandez, M., Noelle, R.J. & Waldschmidt, T.J. Identification of murine germinal center B cell subsets defined by the expression of surface isotypes and differentiation antigens. *J. Immunol.* **164**, 5729–5738 (2000).
21. Maeda, K. *et al.* Murine follicular dendritic cells and low affinity Fc receptors for IgE (FcεRII). *J. Immunol.* **148**, 2340–2347 (1992).
22. Cyster, J.G. *et al.* Follicular stromal cells and lymphocyte homing to follicles. *Immunol. Rev.* **176**, 181–193 (2000).
23. Vonderheide, R.H. & Hunt, S.V. Does the availability of either B cells or CD4$^+$ cells limit germinal centre formation? *Immunology* **69**, 487–489 (1990).
24. Tamamura, H. *et al.* Enhancement of the T140-based pharmacophores leads to the development of more potent and bio-stable CXCR4 antagonists. *Org. Biomol. Chem.* **1**, 3663–3669 (2003).
25. Strasser, A. *et al.* Enforced BCL2 expression in B-lymphoid cells prolongs antibody responses and elicits autoimmune disease. *Proc. Natl. Acad. Sci. USA* **88**, 8661–8665 (1991).
26. Secord, E.A., Edington, J.M. & Thorbecke, G.J. The Eμ-bcl-2 transgene enhances antigen-induced germinal center formation in both BALB/c and SJL mice but causes age-dependent germinal center hyperplasia only in the lymphoma-prone SJL strain. *Am. J. Pathol.* **147**, 422–433 (1995).
27. Smith, K.G. *et al.* Bcl-2 transgene expression inhibits apoptosis in the germinal center and reveals differences in the selection of memory B cells and bone marrow antibody-forming cells. *J. Exp. Med.* **191**, 475–484 (2000).
28. Hargreaves, D.C. *et al.* A coordinated change in chemokine responsiveness guides plasma cell movements. *J. Exp. Med.* **194**, 45–56 (2001).
29. Okada, T. *et al.* Chemokine requirements for B cell entry to lymph nodes and Peyer's patches. *J. Exp. Med.* **196**, 65–75 (2002).
30. Krug, A. *et al.* IFN-producing cells respond to CXCR3 ligands in the presence of CXCL12 and secrete inflammatory chemokines upon activation. *J. Immunol.* **169**, 6079–6083 (2002).
31. Casamayor-Palleja, M. *et al.* Expression of macrophage inflammatory protein-3alpha, stromal cell-derived factor-1, and B-cell-attracting chemokine-1 identifies the tonsil crypt as an attractive site for B cells. *Blood* **97**, 3992–3994 (2001).

32. Amara, A. *et al.* Stromal cell-derived factor-1alpha associates with heparan sulfates through the first β-strand of the chemokine. *J. Biol. Chem.* **274**, 23916–23925 (1999).
33. Nieuwenhuis, P. & Opstelten, D. Functional anatomy of germinal centers. *Am. J. Anat.* **170**, 421–435 (1984).
34. Wehrli, N. *et al.* Changing responsiveness to chemokines allows medullary plasmablasts to leave lymph nodes. *Eur. J. Immunol.* **31**, 609–616 (2001).
35. Guinamard, R. *et al.* B cell antigen receptor engagement inhibits stromal cell-derived factor (SDF)-1α chemotaxis and promotes protein kinase C (PKC)-induced internalization of CXCR4. *J. Exp. Med.* **189**, 1461–1466 (1999).
36. Marchese, A. & Benovic, J.L. Agonist-promoted ubiquitination of the G protein-coupled receptor CXCR4 mediates lysosomal sorting. *J. Biol. Chem.* **276**, 45509–45512 (2001).
37. Balogh, P., Aydar, Y., Tew, J.G. & Szakal, A.K. Appearance and phenotype of murine follicular dendritic cells expressing VCAM-1. *Anat. Rec.* **268**, 160–168 (2002).
38. Egawa, T. *et al.* The earliest stages of B cell development require a chemokine stromal cell-derived factor/pre-B cell growth-stimulating factor. *Immunity* **15**, 323–334 (2001).
39. Ma, Q. *et al.* Impaired B-lymphopoiesis, myelopoiesis, and derailed cerebellar neuron migration in CXCR4- and SDF-1-deficient mice. *Proc. Natl. Acad. Sci. USA* **95**, 9448–9453 (1998).
40. Zou, Y.R., Kottmann, A.H., Kuroda, M., Taniuchi, I. & Littman, D.R. Function of the chemokine receptor CXCR4 in haematopoiesis and in cerebellar development. *Nature* **393**, 595–599 (1998).
41. Ara, T. *et al.* A role of CXC chemokine ligand 12/stromal cell-derived factor-1/pre-B cell growth stimulating factor and its receptor CXCR4 in fetal and adult T cell development *in vivo*. *J. Immunol.* **170**, 4649–4655 (2003).
42. Plotkin, J., Prockop, S.E., Lepique, A. & Petrie, H.T. Critical role for CXCR4 signaling in progenitor localization and T cell differentiation in the postnatal thymus. *J. Immunol.* **171**, 4521–4527 (2003).
43. Martin, C. *et al.* Chemokines acting via CXCR2 and CXCR4 control the release of neutrophils from the bone marrow and their return following senescence. *Immunity* **19**, 583–593 (2003).
44. Bleul, C.C., Fuhlbrigge, R.C., Casasnovas, J.M., Aiuti, A. & Springer, T.A. A highly efficacious lymphocyte chemoattractant, stromal cell-derived factor 1 (SDF-1). *J. Exp. Med.* **184**, 1101–1109 (1996).
45. Hernandez, P.A. *et al.* Mutations in the chemokine receptor gene CXCR4 are associated with WHIM syndrome, a combined immunodeficiency disease. *Nat. Genet.* **34**, 70–74 (2003).
46. Luther, S.A., Gulbranson-Judge, A., Acha-Orbea, H. & MacLennan, I.C. Viral superantigen drives extrafollicular and follicular B cell differentiation leading to virus-specific antibody production. *J. Exp. Med.* **185**, 551–562 (1997).
47. Ngo, V.N., Tang, H.L. & Cyster, J.G. Epstein-Barr virus-induced molecule 1 ligand chemokine is expressed by dendritic cells in lymphoid tissues and strongly attracts naive T cells and activated B cells. *J. Exp. Med.* **188**, 181–191 (1998).
48. Cinamon, G. *et al.* Sphingosine 1-phosphate receptor 1 promotes B cell localization in the splenic marginal zone. *Nat. Immunol.* **5**, 713–720 (2004).

Identification of a CXCR4 antagonist, a T140 analog, as an anti-rheumatoid arthritis agent

Hirokazu Tamamura[a,*], Miho Fujisawa[b], Kenichi Hiramatsu[a], Makiko Mizumoto[a], Hideki Nakashima[c], Naoki Yamamoto[d], Akira Otaka[a], Nobutaka Fujii[a,*]

[a] *Graduate School of Pharmaceutical Sciences, Kyoto University, Sakyo-ku, Kyoto 606-8501, Japan*
[b] *Takeda Chemical Industries, Ltd., Pharmaceutical Research Division, Yodogawa-ku, Osaka 532-8686, Japan*
[c] *School of Medicine, St. Marianna University, Miyamae-ku, Kawasaki 216-8511, Japan*
[d] *School of Medicine, Tokyo Medical and Dental University, Bunkyo-ku, Tokyo 113-8519, Japan*

Received 24 March 2004; revised 7 May 2004; accepted 11 May 2004

Available online 7 June 2004

Edited by Beat Imhof

Abstract Several recent papers support the involvement of an interaction between stromal cell-derived factor-1 (SDF-1/CXCL12) and its receptor, chemokine receptor CXCR4, in memory T cell migration in the inflamed rheumatoid arthritis (RA) synovium. Analogs of the 14-mer peptide T140 were previously found to be specific CXCR4 antagonists that were characterized as not only HIV-entry inhibitors but also anti-cancer-metastatic agents. In this study, a T140 analog, 4F-benzoyl-TN14003, was proven to inhibit CXCL12-mediated migration of human Jurkat cells and mouse splenocyte in a dose-dependent manner in vitro (IC_{50} = 0.65 and 0.54 nM, respectively). Furthermore, slow release administration by subcutaneous injection (s.c.) of 4F-benzoyl-TN14003 using an Alzet osmotic pump significantly suppressed the delayed-type hypersensitivity response induced by sheep red blood cells in mice, and significantly ameliorated clinical severity in collagen-induced arthritis in mice. As such, T140 analogs might be attractive lead compounds for chemotherapy of RA.

Keywords: CXCR4 antagonist; Rheumatoid arthritis; T140; Collagen-induced arthritis; Delayed-type hypersensitivity

1. Introduction

Inflammatory cytokines, such as IL-1, IL-6, IFN-γ and tumor necrosis factor (TNF)-α, and activation markers play a central role in the chronic rheumatoid arthritis (RA) synovium [1]. Development of biological drugs targeting these cytokines, such as humanized monoclonal antibodies, has produced promising results in clinical therapy of RA patients. However, this therapy has not yet reached a stage of perfection, and development of other drugs with novel action mechanisms that are independent of the above cytokine's functions, is required for the improvement of RA chemotherapy. Intrinsically, RA is caused by the $CD4^+$ memory T cell accumulation in the inflamed synovium. Nanki et al. [2] reported that the memory T cells highly express a chemokine receptor CXCR4, and that the concentration of stromal cell-derived factor-1 (SDF-1/CXCL12), an endogenous ligand of CXCR4, is extremely high in the synovium of RA patients compared to controls. They also found that CXCL12 stimulates migration of the memory T cells and inhibits T cell apoptosis, suggesting that the CXCL12–CXCR4 interaction plays an important role in T cell accumulation in the RA synovium. Since chemokine CXCL12 [3–6] is independent of the inflammatory cytokines such as TNF-α, in terms of its expression and action, development of substances that inhibit the CXCL12–CXCR4 interaction might be promising as drugs. We have developed several CXCR4 antagonists, T22 (an 18-mer peptide) [7], T140 (a 14-mer) [8] and FC131 (a cyclic pentapeptide) [9]. These peptides have inhibitory activity against entry of T-cell line-tropic (X4-) HIV-1 into target cells [7,10,11] as well as against cancer metastasis and progression in breast cancer [12], pancreatic cancer [13,14], melanoma [15], acute lymphoblastic leukemia [16], small cell lung cancer [17], etc. In this study, we investigated whether a bio-stable T140 analog, 4F-benzoyl-TN14003 [18], shows anti-RA activity in the following experiments: inhibition assays of Jurkat cell/splenocyte migration mediated by CXCL12 in vitro, the delayed-type hypersensitivity (DTH) response induced by sheep red blood cells (SRBC) in vivo and collagen-induced arthritis (CIA) in vivo.

2. Material and methods

2.1. Material

4F-benzoyl-TN14003 [4-fluorobenzoyl–Arg–Arg–Nal–Cys–Tyr–Cit–Lys–D–Lys–Pro–Tyr–Arg–Cit–Cys–Arg–NH_2, a disulfide bond between Cys^4–Cys^{13}, Nal = L-3-(2-naphthyl)alanine, Cit = L-citrulline] was previously synthesized [18,19].

2.2. Migration assay of human Jurkat cells

Human Jurkat cells were obtained from the American Type Culture Collection (Manassas, VA, USA), and cultured in RPMI-1640 medium (BioWhittaker, Walkersville, MD, USA) supplemented with 10% fetal calf serum (BioWhittaker).

Jurkat cells (2.5×10^6 cells/ml) were pre-incubated with various concentrations of 4F-benzoyl-TN14003 at 37 °C for 30 min. Then 200 μl of this suspension was placed into Transwell (Corning-Costar, Cambridge, MA, USA) culture inserts within 24-well culture plates containing 600 μl of assay medium (RPMI-1640/0.5% BSA/50 mmol/l HEPES) with 10 ng/ml human CXCL12 (Genzyme Techne, Minneapolis, MN, USA). The plates were incubated at 37 °C for 4 h in a humidified 5% CO_2 incubator. After the incubation, the culture inserts

* Corresponding authors. Fax: +81-75-753-4570.
E-mail addresses: tamamura@pharm.kyoto-u.ac.jp (H. Tamamura), nfujii@pharm.kyoto-u.ac.jp (N. Fujii).

0014-5793/$22.00
doi:10.1016/j.febslet.2004.05.056

were removed and migrated cells from the inserts into the wells were counted using a Coulter counter. Percent migration was based on the total initial input per well.

2.3. Mouse splenocyte preparation and migration assay

Spleens were isolated from BALB/c mice (male, Charles River, Yokohama, Japan), and single-cell suspensions prepared from spleens were incubated in RBC lysing buffer (Immuno-Biological Laboratories, Fujioka, Japan), washed twice with PBS and then resuspended in assay medium.

Chemotaxis was measured in a 2.5-h Transwell migration assay as described above. Recombinant mouse CXCL12 (100 ng/ml, PeproTech, London, UK) was added to the wells in chemotaxis medium, and 1×10^7 cells were added to the Transwell inserts. Migrated cells were counted with a Coulter counter.

2.4. Inhibition assay of the mouse DTH response

SRBC were washed twice with saline, and then resuspended in saline. BALB/c mice (male 6 weeks, Charles River) were sensitized with a subcutaneous injection of 5×10^7 SRBC in 50 μl of saline into the left hind footpad. Five days later, mice were challenged by subcutaneously injecting 1×10^8 SRBC in 50 μl of saline into the right hind footpad. The thickness of the right hind paw was measured with a micrometer (Mitutoyo, CD-15B, Kawasaki, Japan) before treatment and 24 h after challenge. The DTH reaction was expressed as the swelling of the right footpad.

2.5. Induction and evaluation of CIA

Bovine type II collagen (CII, Collagen Research Center, Tokyo, Japan) was dissolved in 0.05 mol/l acetic acid to a concentration of 2 mg/ml, and the emulsion was prepared with an equal volume of Freund's complete adjuvant (Difco, Detroit, MI, USA).

Six week-old male DBA/1J mice (Charles River) were injected intradermally at the base of the tail with a volume of 50 μl of the above emulsion. Twenty-one days after immunization, mice were given booster shots with the CII emulsion in the same manner. Following this injection, mice were evaluated for the incidence and the severity of arthritis, body weight and the thickness of the hind ankles, twice a week. At the end of the experimental period (2 weeks after the second injection), sera were obtained and the weights of the 4 limbs were measured.

The clinical severity of the arthritis was graded on a scale of 0–3 for each paw as follows: 0, normal; 1, swelling of one digit or mild swelling of the paw; 2, swelling of multiple digits or moderate swelling of the entire paw; 3, severe swelling of the entire paw. Each mouse could achieve a maximum score of 12.

2.6. Measurement of serum anti-bovine CII antibody

Levels of serum anti-bovine CII IgG2a antibody were measured using an ELISA assay. 96-well immunoplates were coated with bovine CII (10 μg/ml in PBS) and incubated at 4 °C overnight. Non-specific binding was blocked with PBS containing 10% FCS for 2 h. Mouse serum samples diluted with 10% FCS in PBS (1:1000) were added to the wells and incubated at room temperature for 2 h. Horseradish peroxidase-conjugated rat anti-mouse IgG2a antibody (1:1000 diluted, Zymed Laboratories, South San Francisco, CA, USA) was added and incubated for 1 h. 3,3′,5,5′-Tetramethylbenzidine (TMB) substrate solution (DAKO A/S, Glostrup, Denmark) was added and allowed to react for 30 min. The reaction was stopped by the addition of an equal volume of 1 mol/l H_2SO_4, and the optical density at 450 nm was measured using a microplate reader (Labsystems MultiscanMS, Helsinki, Finland). For this ELISA, the wells were washed with PBS containing 0.1% Tween 20 before each step.

2.7. Drug administration

4F-benzoyl-TN14003 was dissolved in PBS, and subcutaneously administered using Alzet osmotic pumps (DURECT Corp., Cupertino, CA, USA), which were implanted dorsalaterally under the skin at the day before immunization (DTH) or the booster (CIA). In the experiment of DTH and CIA, #1007D pumps (delivering 4.8, 24 and 120 μg/day of 4F-benzoyl-TN14003 for 7 days) and # 2002 ones (delivering 120 μg of 4F-benzoyl-TN14003 daily for 14 days) were used, respectively. Indomethacin (1 mg/kg, Sigma Chemicals Co., St. Louis, MO, USA), methotrexate (3 mg/kg, Wako Pure Chemical Industries, Ltd, Osaka, Japan) and FK-506 (10 mg/kg, purified in Takeda Chemical Industries, Ltd, Osaka, Japan) were orally administered once daily for 2 weeks from the day of booster. These drugs were suspended in a 0.5% methylcellulose solution.

2.8. Statistical analysis

The values were represented as the means ± S.E. Statistical differences were determined using an analysis of variance (ANOVA, SAS software, version 6.1, SAS Institute, Cary, NC, USA). Results of DTH were assessed with the one-tailed Williams' test. A value of $P \leqslant 0.025$ was considered statistically significant. In the experiment involving CIA, unpaired or paired *t*-test were applied when only two values sets were compared. When data involved three or more groups, statistical analysis was performed using Dunnett's test. Clinical scores for each group were compared using the non-parametric Steel test or the Wilcoxon rank-sum test. The level of significance was defined as $P \leqslant 0.05$ and $P \leqslant 0.01$.

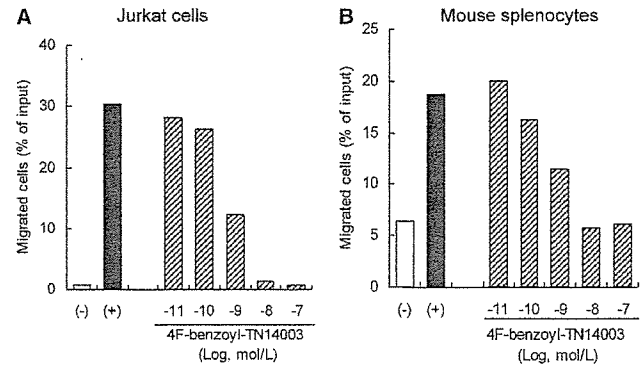

Fig. 1. Effects of 4F-benzoyl-TN14003 on CXCL12-induced migration of human Jurkat cells (A) and mouse splenocytes (B). Both cells were treated by CXCL12 (human CXCL12 10 ng/ml for Jurkat cells, mouse CXCL12 100 ng/ml for splenocytes) and various concentrations of 4F-benzoyl-TN14003. Control migrating cells in the absence and presence of CXCL12 are shown as (–) and (+), respectively. Data are expressed as means ($n = 2$).

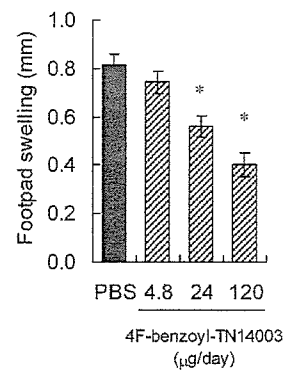

Fig. 2. Inhibition of the mouse DTH response by 4F-benzoyl-TN14003. The gain of thickness of right footpad by swelling 24 h after challenge was measured by a micrometer. PBS (control models) or 4F-benzoyl-TN14003 (4.8, 24 or 120 μg/day) was administered by s.c. injection using an Alzet pump from the day before immunization. Data are expressed as means ± S.E. ($n = 7$). * $P \leqslant 0.025$ (Williams' test).

3. Results

3.1. Inhibition of migration of human Jurkat cells and mouse splenocytes

Both human Jurkat cells and mouse splenocytes express CXCR4 on their surfaces [12,20]. CXCL12 (10 ng/ml = 1.1 nM for Jurkat cells, 100 ng/ml = 11 nM for splenocytes) dramatically enhanced the migration of Jurkat cells and splenocytes, as compared to control (absence of CXCL12, Fig. 1). 4F-benzoyl-TN14003 inhibited CXCL12-induced migration of these cells in a dose-dependent manner. At a concentration of 10 nM, 4F-benzoyl-TN14003 showed approximately 100% inhibition of cell migration induced by CXCL12 (1.1 nM for Jurkat cells, 11 nM for splenocytes). The IC_{50} values were determined to be 0.65 nM and 0.54 nM, respectively.

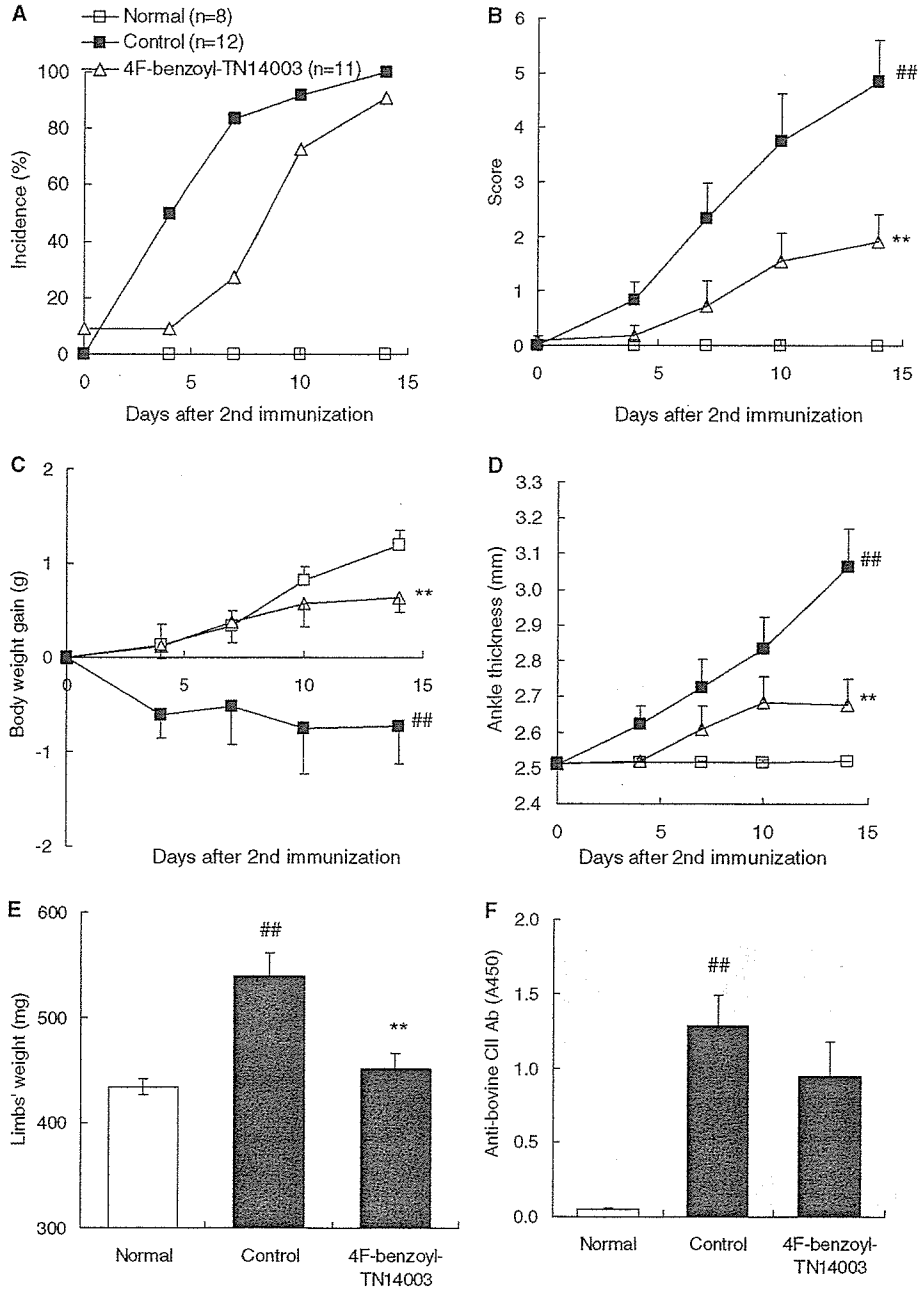

Fig. 3. Suppression of CIA in mice by 4F-benzoyl-TN14003. The incidence (A) and the score expressing the clinical severity (B) of arthritis were evaluated, and body weight (C) and the thickness of the hind ankles (D) were measured after the second immunization twice a week. The weights of 4 limbs were measured 2 weeks after the second immunization (E). Levels of anti-bovine CII IgG2a antibody in serum, which was obtained 2 weeks after the second immunization, were measured by ELISA (F). PBS (control models, $n = 12$) or 4F-benzoyl-TN14003 (120 μg/day, $n = 11$) was administered by s.c. injection using an Alzet pump from the day before the second immunization. In normal models ($n = 8$), mice were not immunized. Data are expressed as means ± S.E. $^{\#\#}P \leqslant 0.01$ (*t*-test): comparison with normal models, $^{**}P \leqslant 0.01$ (*t*-test): comparison with control models (Scores were compared by non-parametric Steel test).

3.2. Reduction of the DTH reaction in mice by subcutaneous administration of 4F-benzoyl-TN14003 using Alzet osmotic pumps

The SRBC-induced DTH reaction in mice was adopted as an in vivo experimental model of the cellular immune response for evaluation of 4F-benzoyl-TN14003 activity. The DTH reaction was estimated as the gain of right footpad thickness from swelling, 24 h after challenge. Seven mice were administered PBS as control models and showed significant footpad swelling (Fig. 2). Twenty one mice were administered 4F-benzoyl-TN14003 by s.c. injection using Alzet pumps (delivering 4.8, 24 and 120 μg/day, each for 7 mice) beginning from the day before immunization. Treated mice showed a dose-dependent suppression of swelling, as compared to control mice. The 24 and 120 μg daily injections showed inhibitory percentages of 31% and 51%, respectively. 4F-benzoyl-TN14003 significantly reduced the DTH reaction in mice.

3.3. Suppression of CIA in mice by subcutaneous administration of 4F-benzoyl-TN14003 using Alzet osmotic pumps

In the next phase, CIA was adopted to provide a second in vivo mouse model of this pathogenesis. During the 2 weeks after the CII emulsion booster, the following data were collected: the arthritis incidence, the scores expressing the severity, the body weight and thickness of the hind ankles were observed twice a week; the 4 limbs' weights and the serum anti-bovine CII antibodies were measured on the 14th day. Eleven mice were administered 4F-benzoyl-TN14003 by s.c. injection using Alzet pumps (delivering 120 μg/day), beginning from the day before the booster. Twelve mice were administered PBS as control models. Eight mice were not immunized as normal models. After observation for 14 days, 4F-benzoyl-TN14003-treated mice showed significant suppression of several symptoms of arthritis (score increase, body weight loss, ankle swelling and limbs' weight gain) as compared to the control mice that developed arthritis (Figs. 3 and 4). 4F-benzoyl-TN14003-treated mice also showed an apparent suppression of the extreme increase in levels of serum anti-bovine CII IgG2a antibody observed for the control group (Fig. 3F).

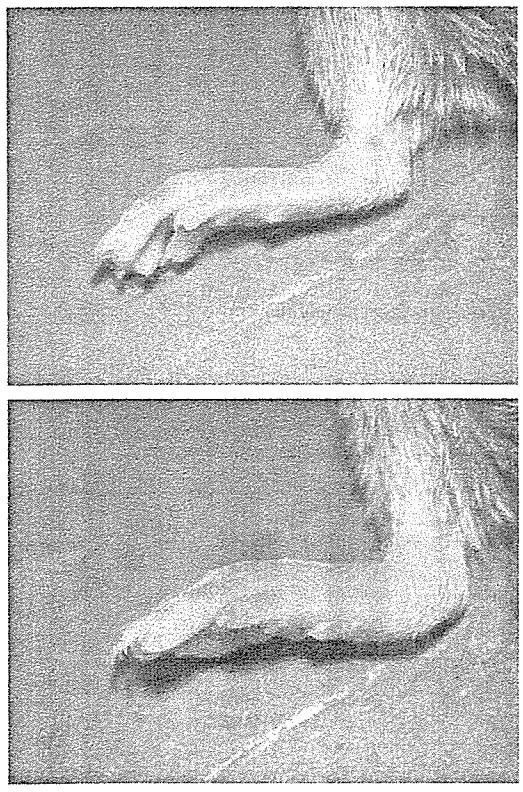

Fig. 4. Reduction of ankle swelling in mouse CIA by 4F-benzoyl-TN14003. Representative hind ankles of mice 2 weeks after the second immunization are shown. *Upper*, 4F-benzoyl-TN14003 was administered by s.c. injection using an Alzet pump from the day before the second immunization; *Lower*, PBS was administered as control models.

In a further comparative study, indomethacin [21] (1 mg/kg), methotrexate [22] (3 mg/kg) and FK-506 [23] (10 mg/kg), which are clinically used for treatment of RA patients or are known as anti-RA agents, were orally administered once daily for 2 weeks from the day of the booster (Fig. 5). These treated mice showed significant suppression of ankle swelling and limb weight gain, and an apparent suppression of marked increases in arthritis scores and anti-bovine CII antibody levels, remarkably similar to the results with 4F-benzoyl-TN14003. Therefore, 4F-benzoyl-TN14003 can be seen to possess inhibitory activity against RA symptoms, comparable to these known drugs.

4. Discussion

Chemokines constitute a chemotactic cytokine family that attract and induce migration of leukocytes, playing a fundamental role in the physiology of inflammation. CXCL12 is a chemokine that recognizes CXCR4. CXCR4 also has significant involvement in several pathological conditions, including AIDS [24], cancer [12–17,25] and RA [2]. The pathological importance of CXCR4 derives from its initial identification as the second receptor involved in the X4-HIV-1 entry into T cells [24]. According to recent reports, CXCL12 induces migration of several types of cancer cells via CXCR4 on their cell surfaces, causing cancer metastasis and progression [12–17,25]. Furthermore, the CXCL12/CXCR4 axis is thought to play an important role in the rheumatoid T cell accumulation in RA, as described in Section 1 [2]. Thus, CXCR4 represents an important therapeutic target for these diseases. We have previously developed several CXCR4 antagonists, T22, T140, 4F-benzoyl-TN14003 and FC131, which have strong anti-HIV-1 and anti-cancer metastatic activities, as described in Section 1 [7–17]. De Clercq's group reported another CXCR4 antagonist, AMD3100, which also has strong anti-HIV-1 activity [26]. Recently, he and his colleagues have found that AMD3100 inhibits autoimmune joint inflammation in IFN-γ receptor-deficient mice, and that AMD3100 interferes with cellular DTH reaction, but not with the humoral immune response to CII in CIA, as assessed by measuring anti-CII antibody levels [20]. In this study, we investigated whether 4F-benzoyl-TN14003 shows anti-RA activity by assessing its effects on humoral and cellular immunity.

We previously reported that 4F-benzoyl-TN14003 has strong binding capacity to CXCR4, as shown by inhibition of [^{125}I]-CXCL12 binding to CXCR4-expressing human Jurkat cells ($IC_{50} = 0.99$ nM) [12]. In this study, 4F-benzoyl-TN14003 was clearly shown to inhibit CXCL12-induced migration of Jurkat cells in a dose-dependent manner at subnanomolar levels, and also to inhibit mouse splenocyte migration induced by CXCL12. These results suggest that the activity of this com-

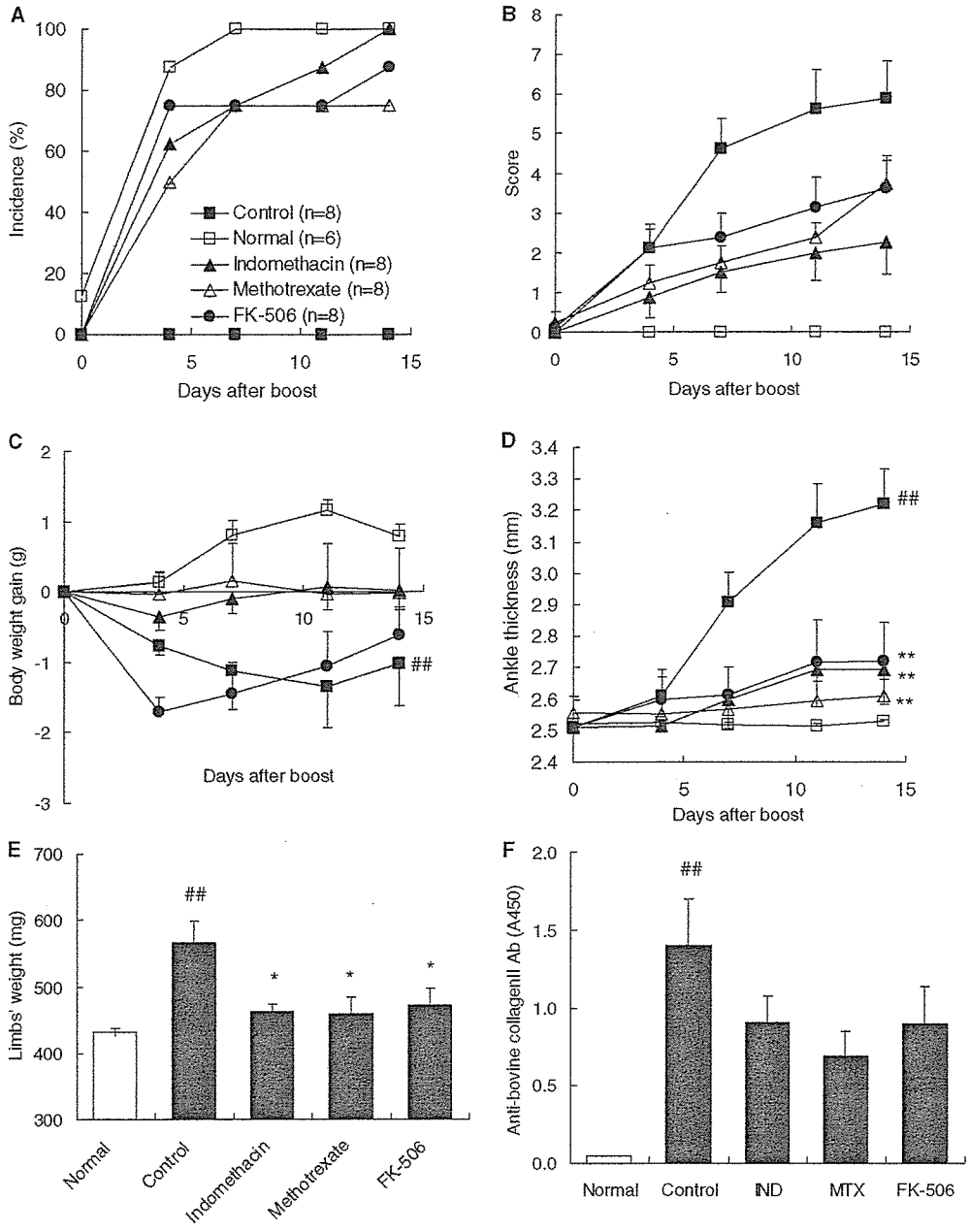

Fig. 5. Suppression of CIA in mice by known drugs. Efficacies of drugs were evaluated in the same way as in the experiments of Fig. 3 (A–F). PBS (control models, $n = 8$), indomethacin (1 mg/kg, $n = 8$), methotrexate (3 mg/kg, $n = 8$) or FK-506 (10 mg/kg, $n = 8$) was orally administered from the day of the second immunization once daily for 2 weeks. In normal models ($n = 6$), mice were not immunized. Data are expressed as means ± S.E. $^{\#\#}P \leqslant 0.01$ (t-test): comparison with normal models, $^{*}P \leqslant 0.05$ and $^{**}P \leqslant 0.01$ (Dunnett's test): comparison with control models.

pound is species independent, possibly due to the close homology of human and mouse CXCR4 [27]. Evaluation of the inhibitory activity of 4F-benzoyl-TN14003 against CXCL12-induced migration of CXCR4-expressing T cells suggests that 4F-benzoyl-TN14003 inhibits CXCL12-stimulated migration of memory T cells, thereby suppressing accumulation of T cells caused by inhibition of their apoptosis in the inflamed synovium of RA patients. Therefore, we investigated the inhibitory effects of 4F-benzoyl-TN14003 against RA using two mouse experimental models: the DTH response and CIA.

To evaluate the effect of 4F-benzoyl-TN14003 on cellular immunity, the DTH reactivity induced by SRBC was examined in mice. Subcutaneous administration of 4F-benzoyl-TN14003 using Alzet osmotic pumps significantly suppressed the footpad swelling. This indicates that 4F-benzoyl-TN14003 interferes with cellular immunity such as DTH, suggesting that CXCR4 might play an important role in cellular immunity.

Next, the activity of 4F-benzoyl-TN14003 was assessed in the CIA experiment, an RA animal model. The levels of several CIA symptoms were significantly lower in 4F-benzoyl-TN14003-treated mice than those in PBS-treated mice (arthritic control mice). Serum levels of the anti-CII IgG2a anti-body were also apparently lower in 4F-benzoyl-TN14003-treated mice. 4F-benzoyl-TN14003 therefore interferes with the humoral immune

response to CII, in contrast to AMD3100 [20]. The differences in the actions of AMD3100 and 4F-benzoyl-TN14003 in humoral CIA immunity might be explained by a difference in the binding sites of these CXCR4 antagonists [28] or by differences in the CIA models that were used.

In conclusion, the present results suggest that a bio-stable T140 analog, 4F-benzoyl-TN14003, inhibits the migration and accumulation of rheumatoid T cells through a specific binding to CXCR4 in competition with CXCL12. This compound interfered with cellular and humoral immune responses in experimental arthritis models in mice, and showed inhibitory effects against the CIA development at levels comparable to, or above those of known drugs. Since T140 is an inverse agonist, which has no CXCL12-like agonistic activity [29], it and its analogs have the potential of becoming promising agents for RA chemotherapy as well as for AIDS and cancer chemotherapy.

Acknowledgements: This work was supported in part by a 21st Century COE Program "Knowledge Information Infrastructure for Genome Science", a Grant-in-Aid for Scientific Research from the Ministry of Education, Culture, Sports, Science and Technology, Japan and a Health and Labour Sciences Research Grant on Health Sciences focusing on Drug Innovation. The authors wish to thank Prof. Scott McN. Sieburth, Department of Chemistry, Temple University, PA, USA for proofreading the manuscript and providing useful comments.

References

[1] Nanki, T. and Lipsky, P.E. (2000) Arthritis Res. 2, 415–423.
[2] Nanki, T., Hayashida, K., El-Gabalawy, H.S., Suson, S., Shi, K., Girschick, H.J., Yavuz, S. and Lipsky, P.E. (2000) J. Immunol. 165, 6590–6598.
[3] Nagasawa, T., Kikutani, H. and Kishimoto, T. (1994) Proc. Natl. Acad. Sci. USA 91, 2305–2309.
[4] Bleul, C.C., Farzan, M., Choe, H., Parolin, C., Clark-Lewis, I., Sodroski, J. and Springer, T.A. (1996) Nature 382, 829–833.
[5] Oberlin, E., Amara, A., Bachelerie, F., Bessia, C., Virelizier, J.-L., Arenzana-Seisdedos, F., Schwartz, O., Heard, J.-M., Clark-Lewis, I., Legler, D.F., Loetscher, M., Baggiolini, M. and Moser, B. (1996) Nature 382, 833–835.
[6] Tashiro, K., Tada, H., Heilker, R., Shirozu, M., Nakano, T. and Honjo, T. (1993) Science 261, 600–603.
[7] Murakami, T., Nakajima, T., Koyanagi, Y., Tachibana, K., Fujii, N., Tamamura, H., Yoshida, N., Waki, M., Matsumoto, A., Yoshie, O., Kishimoto, T., Yamamoto, N. and Nagasawa, T. (1997) J. Exp. Med. 186, 1389–1393.
[8] Tamamura, H., Xu, Y., Hattori, T., Zhang, X., Arakaki, R., Kanbara, K., Omagari, A., Otaka, A., Ibuka, T., Yamamoto, N., Nakashima, H. and Fujii, N. (1998) Biochem. Biophys. Res. Commun. 253, 877–882.
[9] Fujii, N., Oishi, S., Hiramatsu, K., Araki, T., Ueda, S., Tamamura, H., Otaka, A., Kusano, S., Terakubo, S., Nakashima, H., Broach, J.A., Trent, J.O., Wang, Z. and Peiper, S.C. (2003) Angew. Chem. Int. Ed. Engl. 42, 3251–3253.
[10] Murakami, T., Zhang, T.-Y., Koyanagi, Y., Tanaka, Y., Kim, J., Suzuki, Y., Minoguchi, S., Tamamura, H., Waki, M., Matsumoto, A., Fujii, N., Shida, H., Hoxie, J., Peiper, S.C. and Yamamoto, N. (1999) J. Virol. 73, 7489–7496.
[11] Xu, Y., Tamamura, H., Arakaki, R., Nakashima, H., Zhang, X., Fujii, N., Uchiyama, T. and Hattori, T. (1999) AIDS Res. Hum. Retroviruses 15, 419–427.
[12] Tamamura, H., Hori, A., Kanzaki, N., Hiramatsu, K., Mizumoto, M., Nakashima, H., Yamamoto, N., Otaka, A. and Fujii, N. (2003) FEBS Lett. 550, 79–83.
[13] Koshiba, T., Hosotani, R., Miyamoto, Y., Ida, J., Tsuji, S., Nakamura, S., Kawaguchi, M., Kobayashi, H., Doi, R., Hori, T., Fujii, N. and Imamura, M. (2000) Clin. Cancer Res. 6, 3530–3535.
[14] Mori, T., Doi, R., Koizumi, M., Toyoda, E., Ito, D., Kami, K., Masui, T., Fujimoto, K., Tamamura, H., Hiramatsu, K., Fujii, N. and Imamura, M. (2004) Mol. Cancer Ther. 3, 29–37.
[15] Murakami, T., Maki, W., Cardones, A.R., Fang, H., Tun Kyi, A., Nestle, F.O. and Hwang, S.T. (2002) Cancer Res. 62, 7328–7334.
[16] Juarez, J., Bradstock, K.F., Gottlieb, D.J. and Bendall, L.J. (2003) Leukemia 17, 1294–1300.
[17] Burger, M., Glodek, A., Hartmann, T., Schmitt-Graft, A., Seilberstein, L.E., Fujii, N., Kipps, T.J. and Burger, J.A. (2003) Oncogene 22, 8093–8101.
[18] Tamamura, H., Hiramatsu, K., Mizumoto, M., Ueda, S., Kusano, S., Terakubo, S., Akamatsu, M., Yamamoto, N., Trent, J.O., Wang, Z., Peiper, S.C., Nakashima, H., Otaka, A. and Fujii, N. (2003) Org. Biomol. Chem. 1, 3663–3669.
[19] Tamamura, H., Hiramatsu, K., Kusano, S., Terakubo, S., Yamamoto, N., Trent, J.O., Wang, Z., Peiper, S.C., Nakashima, H., Otaka, A. and Fujii, N. (2003) Org. Biomol. Chem. 1, 3656–3662.
[20] Matthys, P., Hatse, S., Vermeire, K., Wuyts, A., Bridger, G., Henson, G.W., De Clercq, E., Billiau, A. and Schols, D. (2001) J. Immunol. 167, 4686–4692.
[21] Hart, F.D. and Huskisson, E.C. (1984) Drugs 24, 232–255.
[22] Arndt, U., Rittmeister, M. and Moller, B. (2003) Orthopade 32, 1095–1103.
[23] Magari, K., Nishigaki, F., Sasakawa, T., Ogawa, T., Miyata, S., Ohkubo, Y., Mutoh, S. and Goto, T. (2003) Inflamm. Res. 52, 524–529.
[24] Feng, Y., Broder, C.C., Kennedy, P.E. and Berger, E.A. (1996) Science 272, 872–877.
[25] Müller, A., Homey, B., Soto, H., Ge, N., Catron, D., Buchanan, M.E., McClanahan, T., Murphy, E., Yuan, W., Wagner, S.N., Barrera, J.L., Mohar, A., Verastegui, E. and Zlotnik, A. (2001) Nature 410, 50–56.
[26] Schols, D., Struyf, S., Van Damme, J., Este, J.A., Henson, G. and De Clercq, E. (1997) J. Exp. Med. 186, 1383–1388.
[27] Nagasawa, T., Nakajima, T., Tachibana, K., Iizasa, H., Bleul, C.C., Yoshie, O., Matsushima, K., Yoshida, N., Springer, T.A. and Kishimoto, T. (1996) Proc. Natl. Acad. Sci. USA 93, 14726–14729.
[28] Trent, J.O., Wang, Z., Murray, J.L., Shao, W., Tamamura, H., Fujii, N. and Peiper, S.C. (2003) J. Biol. Chem. 278, 47136–47144.
[29] Zhang, W., Navenot, J.M., Haribabu, B., Tamamura, H., Hiramatu, K., Omagari, A., Pei, G., Manfredi, J.P., Fujii, N., Broach, J.R. and Peiper, S.C. (2002) J. Biol. Chem. 277, 24515–24521.

Journal of Neuroscience Research 76:35–50 (2004)

Stromal Cell-Derived Factor 1-Mediated CXCR4 Signaling in Rat and Human Cortical Neural Progenitor Cells

Hui Peng,[1,2] Yunlong Huang,[1,2] Jeremy Rose,[1,2] David Erichsen,[1,2] Shelley Herek,[1,2] Nobutaka Fujii,[3] Hirokazu Tamamura,[3] and Jialin Zheng[1,2,4]*

[1]Laboratory of Neurotoxicology, the Center for Neurovirology and Neurodegenerative Disorders, University of Nebraska Medical Center, Omaha
[2]Department of Pathology and Microbiology, University of Nebraska Medical Center, Omaha
[3]Graduate School of Pharmaceutical Sciences, Kyoto University, Japan
[4]Department of Pharmacology, University of Nebraska Medical Center, Omaha

Stromal cell-derived factor 1 (SDF-1) and the chemokine receptor CXCR4 are highly expressed in the nervous system. Knockout studies have suggested that both SDF-1 and CXCR4 play essential roles in cerebellar, hippocampal, and neocortical neural cell migration during embryogenesis. To extend these observations, CXCR4 signaling events in rat and human neural progenitor cells (NPCs) were examined. Our results show that CXCR4 is expressed in abundance on rat and human NPCs. Moreover, SDF-1α induced increased NPCs levels of inositol 1,4,5-triphosphate, extracellular signal-regulated kinases 1/2, Akt, c-Jun N-terminal kinase, and intracellular calcium whereas it diminished cyclic adenosine monophosphate. Finally, SDF-1α can induce human NPC chemotaxis in vitro, suggesting that CXCR4 plays a functional role in NPC migration. Both T140, a CXCR4 antagonist, and pertussis toxin (PTX), an inactivator of G protein-coupled receptors, abrogated these events. Ultimately, this study suggested that SDF-1α can influence NPC function through CXCR4 and that CXCR4 is functional on NPC.

Key words: neural progenitor cell; neurogenesis; SDF-1α; CXCR4; intracellular signaling

Chemokines (chemotactic cytokines) constitute a family of low molecular mass (8–11 kDa) structurally related proteins with diverse immune and neural functions (Broxmeyer and Kim, 1999; Youn et al., 2000; Mackay, 2001). Four chemokine subfamilies, C, CC, CXC, and CX3C are distinguished based on the relative position of conserved cysteine residues. Stromal cell-derived factor-1α (SDF-1α, CXCL12) is a member of the C-X-C chemokine subfamily and the only known ligand for the G protein-coupled receptor, CXCR4 (Rossi and Zlotnik, 2000), a co-receptor for the human immunodeficiency virus (HIV) (Berson et al., 1996; Brelot et al., 1997; Youn et al., 2000). The primary structure of SDF-1 is remarkably conserved across species, with only one amino acid difference between human and mouse proteins (Shirozu et al., 1995). Two isoforms of SDF-1, SDF-1α and SDF-1β, differ only by four amino acids at the C-terminus, are generated from a single gene by differential RNA splicing (Shirozu et al., 1995).

CXCR4 and SDF-1 are highly expressed during development in the cerebellum, hippocampus, and neocortex and are also expressed constitutively in the brain during adulthood (Jazin et al., 1997; Ma et al., 1998; Zou et al., 1998; Lu et al., 2001; Stumm et al., 2003). Recent studies suggest that SDF-1α and CXCR4 play an important role in central nervous system (CNS) homeostasis

Abbreviations: AIDS, acquired immunodeficiency syndrome; bFGF, basic fibroblast growth factor; BrdU, bromodeoxyuridine; cAMP, cyclic adenosine monophosphate; CNS, central nervous system; EGF, epidermal growth factor; EGL, external granule cell layer; ERK, extracellular signal-regulated kinases; FBS, fetal bovine serum; FSK, forskolin; GalC, galactocerebroside; GFAP, glial fibrillary acidic protein; HAD, HIV-1-associated dementia; HIVE, HIV-1 encephalitis; IP_3, inositol 1, 4, 5-triphosphate; JNK, c-Jun N-terminal kinase; LIF, lymphocyte inhibitory factor; MAP kinase, mitogen-activated protein kinase; MAP-2, microtubule associated protein-2; MP, mononuclear phagocytes; NeuN, neuron-specific nuclear; NPBM, neuronal progenitor cell basal media; NPC, neuronal progenitor cell; NSF-1, neural survival factor; NPIM, neurosphere initial media; NPMM, neural progenitor cell maintenance media; PKA, protein kinase A; PKB, protein kinase B; PTX, pertussis toxin; SDF-1, stromal cell-derived factor.

Part of this work was presented at the Society for Neuroscience 2002 Annual Meeting, Orlando, FL.

Contract grant sponsor: National Institutes of Health; Contract grant number: R01 NS 41858-01, P20 RR15635-01, P01 NS043985.

*Correspondence to: Dr. Jialin Zheng, Laboratory of Neurotoxicology, Center for Neurovirology and Neurodegenerative Disorders, 985215 Nebraska Medical Center, Omaha, NE 68198-5215.
E-mail: jzheng@unmc.edu

Received 2 October 2003; Revised 10 December 2003; Accepted 12 December 2003

Published online 5 March 2004 in Wiley InterScience (www.interscience.wiley.com). DOI: 10.1002/jnr.20045

(Jazin et al., 1997; Ma et al., 1998; Zou et al., 1998; Bagri et al., 2002; Lu et al., 2002; Stumm et al., 2003). For example, mice with a targeted mutation in CXCR4 or SDF-1α have a defect in migration of cerebellar granule cells (Ma et al., 1998; Zou et al., 1998). The morphology of the hippocampal dentate gyrus (DG) is also altered markedly in CXCR4 mutant mice (Bagri et al., 2002; Lu et al., 2002). Furthermore, mice with a null mutation in CXCR4 or SDF-1 show interneurons that are severely underrepresented in the superficial layers and are ectopically placed in the deep layers of the neocortex (Stumm et al., 2003). Moreover, an in vitro study indicates that SDF-1α incites migration of neuronal precursor cells (NPCs) from the external granule cell layer (EGL) to the internal granular layer (Zhu et al., 2002). This activity indicates a crucial role for SDF-1α/CXCR4 interactions in NPC migration during development.

Neurogenesis, an important step in neural development, may play a vital role in neuronal repair during disease processes (Gage, 2000). Neural stem cells, including early stem cells and late progenitor cells, exist throughout life and can renew and give rise to new neurons, astrocytes, and oligodendrocytes (Alvarez-Buylla et al., 2002; Alvarez-Buylla and Garcia-Verdugo, 2002; Kintner, 2002). Adult neural stem cells exist in many brain structures including the subventricular zone, the dentate gyrus, and the cortex (Gould et al., 1999; Magavi et al., 2000; Gould and Gross, 2002; Stumm et al., 2002, 2003). Exercise, stress, ischemic and excitotoxic brain injuries can affect neurogenesis (Kempermann et al., 1997; Parent et al., 1997; Liu et al., 1998; McTigue et al., 1998; van Praag et al., 1999; Gage, 2000, 2002; Nakatomi et al., 2002).

Although it is clear that CXCR4 is a vital receptor for neuronal development, the role this receptor plays in regulating NPC function and how it could affect neurogenesis during development and pathologic situations requires further study. To further assess the role of CXCR4 in development and perhaps disease, signaling pathways in NPCs derived from rat and human cortexes were investigated. The role of SDF-1α in CXCR4-mediated signaling on NPCs, such as inositol 1,4,5-triphosphate (IP_3) formation, calcium release, cyclic adenosine monophosphate (cAMP) production, and mitogen-activated protein kinase (MAP kinase) activation was determined. Such characterization may provide unique insights into the pathogenesis of neurodegenerative disorders where changes in neural chemotaxis and inflammatory cell signaling events abound.

MATERIALS AND METHODS

Isolation and Culture of Rat Cortical NPCs

NPC cultures were prepared as reported previously, with some modifications (Hazel and Muller, 1997). Briefly, brain cerebral hemispheres were removed from embryonic day (E15) Sprague-Dawley rat embryos (Davis and Temple, 1994; Hazel and Muller, 1997; Jazin et al., 1997; Lazarini et al., 2000), following protocols approved previously by the University of Nebraska Medical Center Institutional Animal Care and Use Committee, and utilizing National Institutes of Health (NIH) ethical guidelines. After removal of the meninges, the tissue was dissociated mechanically to single cells in a Ca^{2+}/Mg^{2+}-free Hank's balanced salt solution (HBSS) and plated at 5×10^6 cells/flask in 10 ml NPC maintenance media (NPMM), neuronal progenitor basal media (NPBM; BioWhittaker, San Diego, CA) supplemented with basic fibroblast growth factor (bFGF; Sigma, St. Louis, MO), Epidermal growth factor (EGF; Sigma) and neural survival factor-1 (NSF-1; BioWhittaker) in T75 flasks coated with poly-D-lysine (Sigma). After 4–5 days in culture, cells were approximately 50% confluent and were passaged by incubating in a Ca^{2+}/Mg^{2+}-free HBSS for 15 min at 37°C and triturated to a single-cell suspension, followed by binding assay, cAMP assay, PI hydrolysis, kinase assays, and calcium flux analysis. Passaged cells that had attached to poly-D-lysine precoated 8-well chamber slides for 24 hr or that differentiated for 7 days were characterized by immunocytochemistry.

Isolation and Culture of Human Cortical NPCs

Human fetal brain tissue (12–16 weeks post-conception) was obtained from elective abortions carried out in full compliance with the University of Nebraska Medical Center (UNMC) and NIH ethical guidelines. The cortex was mechanically dissociated and incubated with 0.25% trypsin for 30 min, neutralized with 10% fetal bovine serum (FBS), further dissociated by titration, washed, and titrated to a single-cell suspension. Cells were seeded at a concentration of 500,000 cells/ml into substrate-free tissue culture flasks and grown as spheres in neurosphere initiation medium (NPIM). Medium consisted of Ex Vivo 15 (BioWhittaker) medium with N2 supplement (Gibco BRL, Carlsbad, CA), bFGF (20 ng/ml), EGF (20 ng/ml), lymphocyte inhibitory factor (LIF; 10 ng/ml), NSF-1 (BioWhittaker), and 60 ng/ml *N*-acetylcysteine (Sigma) as described previously (Schuldiner et al., 2000; Uchida et al., 2000; Monaco et al., 2001). Passaging of these cultures consisted of 15 min trypsin incubation and gentle mechanical dissociation every 14 days. After each passage, the cells were seeded at a concentration of 200,000 cells/ml into substrate-free tissue culture flasks.

Immunocytochemical Detection of NPCs

Passaged cells were cultured in poly-D-lysine-coated 8-well chamber slides at a density of 1×10^4 cells/well. For differentiation studies, cells were allowed to attach in NPMM or NPIM for 24 hr. Media was then exchanged with neurobasal media containing B27 supplement (Gibco BRL) and 5 mM glutamine. Cultures were fed by a 50% media exchange after 3 days. Differentiated cells, after 7 days in culture, or NPCs, after 2 days in culture, were fixed with methanol/acetone (1:1) for 20 min at −20°C and then washed with phosphate-buffered saline (PBS). After being blocked with 2% bovine serum albumin (BSA) and 0.1% Triton X-100 in PBS for 1 hr, NPCs were incubated for 1 hr at room temperature with primary antibodies to nestin (1:100; Chemicon, Temecula, CA), CXCR2 (1:100, monoclonal; R&D Systems), and CXCR4 (1:100, monoclonal, R&D Systems). Differentiated cells were incubated with primary antibodies to β-Tubulin Isotype III (1:400; Sigma) neuronal-specific microtubule-associated protein-2 (MAP-2, 1:100, monoclonal; Chemicon), neuronal nuclei (NeuN, 1:200,